Atmos. Chem. Phys. Discuss., 15, 18691–18746, 2015
www.atmos-chem-phys-discuss.net/15/18691/2015/
doi:10.5194/acpd-15-18691-2015

Atmospheric Chemistry and Physics Discussions

Advantages of city-scale emission inventory for urban air quality research and policy: the case of Nanjing, a typical industrial city in the Yangtze River Delta, China

Y. Zhao[1,2,*], L. Qiu[1,*], R. Xu[1], F. Xie[3], Q. Zhang[4], Y. Yu[5], C. P. Nielsen[6], H. Qin[3], H. Wang[1], X. Wu[1], W. Li[3], and J. Zhang[2,7]

[1]State Key Laboratory of Pollution Control & Resource Reuse and School of the Environment, Nanjing University, 163 Xianlin Ave., Nanjing, Jiangsu 210023, China
[2]Jiangsu Collaborative Innovation Center of Atmospheric Environment and Equipment Technology (CICAEET), Nanjing University of Information Science & Technology, Jiangsu 210044, China
[3]Nanjing Academy of Environmental Protection Science, 175 Huju Rd., Nanjing, Jiangsu 210013, China
[4]Ministry of Education Key Laboratory for Earth System Modeling, Center for Earth System Science, Tsinghua University, Beijing 100084, China

[5]Nanjing Environmental Monitoring Central Station, 175 Huju Rd., Nanjing, Jiangsu 210013, China
[6]Harvard China Project, School of Engineering and Applied Sciences, Harvard University, 29 Oxford St, Cambridge, MA 02138, USA
[7]Jiangsu Provincial Academy of Environmental Science, 176 North Jiangdong Rd., Nanjing, Jiangsu 210036, China
*Y. Zhao and L. Qiu contributed equally to this work.

Received: 08 June 2015 – Accepted: 25 June 2015 – Published: 09 July 2015

Correspondence to: Y. Zhao (yuzhao@nju.edu.cn)

Published by Copernicus Publications on behalf of the European Geosciences Union.

ACPD
15, 18691–18746, 2015

Abstract

With most eastern Chinese cities facing major air quality challenges, there is a strong need for city-scale emission inventories for use in both chemical transport modeling and the development of pollution control policies. In this paper, a high-resolution emission inventory of air pollutants and CO_2 for Nanjing, a typical large city in the Yangtze River Delta, is developed incorporating the best available information on local sources. Emission factors and activity data at the unit or facility level are collected and compiled using a thorough onsite survey of major sources. Over 900 individual plants, which account for 97 % of the city's total coal consumption, are identified as point sources, and all of the emission-related parameters including combustion technology, fuel quality, and removal efficiency of air pollution control devices (APCD) are analyzed. New data-collection approaches including continuous emission monitoring systems and real-time monitoring of traffic flows are employed to improve spatiotemporal distribution of emissions. Despite fast growth of energy consumption between 2010 and 2012, relatively small inter-annual changes in emissions are found for most air pollutants during this period, attributed mainly to benefits of growing APCD deployment and the comparatively strong and improving regulatory oversight of the large point sources that dominate the levels and spatial distributions of Nanjing emissions overall. The improvement of this city-level emission inventory is indicated by comparisons with observations and other inventories at larger spatial scale. Relatively good spatial correlations are found for SO_2, NO_x, and CO between the city-scale emission estimates and concentrations at 9 state-opertated monitoring sites (R = 0.58, 0.46, and 0.61, respectively). The emission ratios of specific pollutants including BC to CO, OC to EC, and CO_2 to CO compare well to top-down constraints from ground observations. The inter-annual variability and spatial distribution of NO_x emissions are consistent with NO_2 vertical column density measured by the Ozone Monitoring Instrument (OMI). In particular, the Nanjing city-scale emission inventory correlates better with satellite observations than the down-scaled Multi-resolution Emission Inventory for China (MEIC) does when emissions from

ACPD
15, 18691–18746, 2015

power plants are excluded. This indicates improvement in emission estimation for sectors other than power generation, notably industry and transportation. High-resolution emission inventory may also provide a basis to consider the quality of instrumental observations. To further improve emission estimation and evaluation, more measurements of both emission factors and ambient levels of given pollutants are suggested; the uncertainties of emission inventories at city scale should also be fully quantified and compared with those at national scale.

1 Introduction

Emission inventories are crucial for atmospheric science research, particularly chemical transport modeling (CTM), and for air quality policymaking that seeks to identify and control pollution sources. Given China's important role in the origins and transport of air pollutants in East Asia and beyond, a number of emission inventories at national scale have been established in recent years. These include the Transport and Chemical Evolution over the Pacific Mission (TRACE-P, Streets et al., 2003), the Intercontinental Chemical Transport Experiment-Phase B (INTEX-B, Zhang et al., 2009), the Regional Emission inventory in ASia (REAS, Ohara et al., 2007; Kurokawa et al., 2013), and the Multi-resolution Emission Inventory for China (MEIC, http://www.meicmodel.org/). Based on "bottom-up" principles and frameworks similar to those described in Streets et al. (2003), more detailed source categories and expanded domestic information on emission factors and activity levels have been integrated into most recent work, yielding improved inter-annual trends in national estimates of anthropogenic air pollutant emissions (e.g., MEIC; Zhao et al., 2012a, b, 2013). Aside from the national-level work, regional emission inventories have also been established with improved understanding of local conditions for key areas with high densities of population, industry, and energy consumption, e.g., the Jing–Jin–Ji region including Beijing and Tianjin (JJJ; S. Wang et al., 2010), the Yangtze River Delta (YRD; Fu et al., 2013; Huang et al., 2011), and the Pearl River Delta (PRD; Zheng et al., 2009).

ACPD
15, 18691–18746, 2015

There is still need for improvement of bottom-up emission inventories, however, particularly at smaller spatial scales. First, data for activity levels and emission factors used in current Chinese inventories come mostly from coarse statistics or surveys at the provincial level, except for select sectors (e.g., power generation, Zhao et al., 2008). Underlying information that is crucial to emission levels (e.g., combustion or manufacturing technologies, fuel qualities, and penetrations and removal efficiencies of various emission control devices) has often been overlooked or assumed to be uniform, inevitably reducing the accuracy and reliability of emission estimates. Without sufficient source-specific information, in particular, it is hard to identify and characterize "super-emitting" sources, which can strongly affect aggregate emission estimates. Second, the spatial and temporal distributions of emissions are often not well characterized. Emissions from most sectors are spatially allocated according to proxies, e.g., population or economic densities. However, the distribution of large sources in China is changing quickly because much industrial production is being relocated out of urban cores, and the correlations between emissions and the usual proxies like population density are getting weaker, particularly in developed cities (Zhang et al., 2012a; Zhao et al., 2013). This introduces error into the spatial allocations. The time distribution of emissions is commonly based on expert judgment, with little reliance on real-time data sources, e.g., continuous emission monitoring systems (CEMS). Finally, some sources that may play important roles in local emissions are often missed in regional emission inventories, e.g., fugitive dust from construction and road transportation, and volatile organic compounds (VOC) from gas stations, mainly due to data limits on such sources. Such limitations weaken capacities to research atmospheric chemistry using inventories as inputs to CTMs, and also undermine the efficacy of pollution control decision-making.

Several studies have illustrated the benefits of city-scale emission inventories that integrate more detailed local information. Timmermans et al. (2013), for example, concluded that the results of NO_2 and PM_{10} simulations were more consistent with observations for Paris when a local emission inventory was used. In the US, model simulations of NO_2 columns based on actual hourly NO_x emissions from CEMS agreed

ACPD
15, 18691–18746, 2015

better with satellite observations than those based on default emission inputs from the U.S. Environmental Protection Agency (USEPA; Kim et al., 2009). In China, vehicle emission inventories resolved at the county level, rather than provincial level, were shown to better support air quality simulations for small regions (Zheng et al., 2014).

China is experiencing frequent severe haze episodes (Zhang et al., 2012b; Wang et al., 2013, 2014; R. Huang et al., 2014). Cities are being required to expand efforts at air pollution control, and use of CTMs for air quality assessment and policy making is becoming more routine. Due in part to weak emission inputs, however, atmospheric simulations for cities are often disappointingly inaccurate (personal communication with Zifa Wang from Institute of Atmospheric Physics, Chinese Academy of Science, 2014). Without integrating more detailed local information, some cities simply downscale a national emission inventory into high-resolution emission inputs for a CTM or develop local inventories based on the same source data and methods used for national ones. Despite improvements from some information (e.g., the precise location of large point sources), the quality and reliability of those inventories have not been well evaluated using, for example, integrated observational data as top-down constraints. Thus the emission estimates introduce large uncertainties into the city-scale air quality simulations.

It should be noted that such improvements in emission inventories for a few megacities, including Beijing and Shanghai, have been driven by air quality planning for major events like the 2008 Summer Olympic Games and 2010 World Expo. During recent years, however, satellite observations have detected that the most significant growth in air pollution (indicated for example by vertical column densities of tropospheric NO_2) across the country is occurring not within such megacities but in the less-developed regions around them, due to faster growth in the economies and emission sources in those areas (Zhang et al., 2012a). This finding highlights the importance of developing and assessing air pollutant emission inventories for regions other than China's much-studied megacities.

ACPD
15, 18691–18746, 2015

We select Nanjing, a typical large city in the YRD, to establish and evaluate a high-resolution emission inventory at city scale. As shown in Fig. S1a in the Supplement, Nanjing is the capital city of Jiangsu Province and the second largest city in central east China following Shanghai, with a total area of 6587 km^2 and population of 8 million in 2012 (NJNBS, 2013). Intensively industrial, Nanjing consumes much more coal than many other Chinese cities with economies of similar size (e.g., Hangzhou, Qingdao, and Shenyang), and in 2012 suffered the highest number of days of haze (226) of all of China's provincial capital cities (data provided by the Nanjing Meteorological Bureau). The share of coal use in primary energy reached 89 % in 2012 (Environmental Statistics, an internal database of the Nanjing Environmental Protection Bureau, NJEPB; NJNBS, 2013), much higher than the national level of 71 % (NBSC, 2013). Large coal consumption and industrial and chemical production have resulted in high emissions of anthropogenic atmospheric pollutants. As the host city of the 2nd Asian Youth Games (AYG) in August 2013, Nanjing undertook various measures to control emissions in industry but allowed construction activities at thousands of sites, leading to large changes in the levels and the temporal and spatial distributions of emissions. Such changes are captured by a comprehensive city-scale emission inventory.

2 Data and methods

2.1 The basic methodology

The annual emissions in Nanjing from 2010 to 2012 are estimated with a bottom-up approach for 10 atmospheric pollutants (SO_2, NO_x, total suspended particulates (TSP), PM_{10}, $PM_{2.5}$, black carbon (BC) or elemental carbon (EC), organic carbon (OC), CO, VOCs, and NH_3) and the greenhouse gas CO_2. At the largest scale, sources fall into six main categories: coal-fired power plants (CPP), industry (IND), transportation (TRA, including on-road and non-road subcategories), the residential and commercial sector (RES, including fossil fuel, biofuel, and biomass open burning subcategories, along

ACPD
15, 18691–18746, 2015

with gas stations for VOC estimation only), agriculture (AGR, including livestock farming and fertilizer use for NH_3 estimation only), and fugitive dust (FUD, including that from construction sites and roads). IND is further divided into cement plants (CEM), iron and steel plants (ISP), refineries and chemical plants (RCP), solvent use (SOL; although some solvent is not used in industry, we include it in this category for classification simplicity) and other industry plants (OIN).

To improve the accuracy and reliability of the city-level emission inventory, new data are collected from various sources and modified methods are applied compared to previous studies, as briefly summarized below.

With sufficient information related to emission estimation now available, more sources can be characterized as point sources in the current inventory. These include power plants (total number in 2012, similarly for subsequent categories: 18), cement plants (23), iron and steel plants (2), chemical plants (173), non-ferrous metal smelters (14), lime plants (9), brick plants (31), factories representing a portion of other industrial sectors (434), and gas-fueling stations (269). The locations of point sources by category are shown in Fig. S1b and c in the Supplement. The annual emissions of point sources are calculated with Eq. (1):

$$E_i = \sum_{j,m} A_{i,j,m} \times \mathrm{EF}_{i,j,m} \times (1 - \eta_{i,j,m}) \quad (1)$$

where i, j and m represent the species, individual plant, and fuel/technology type, respectively; A is the activity level data; EF is the uncontrolled emission factor; and η is removal efficiency of air pollutant control device (APCD).

For all the point sources, information from the Environmental Statistics database and Pollution Source Census (internal data of NJEPB) is collected and compiled to obtain the activity levels (energy consumption or industrial production) and parameters related to emission factors, plant by plant. Moreover, we conduct onsite surveys individually for all of the CPP, CEM, ISP and RCP sources (labeled "key sources" in this paper), to get further information that is crucial for emission estimation but not covered by the

ACPD
15, 18691–18746, 2015

official census or statistics (see details in Sect. 2.2). In 2012, all of the point sources and all of the key sources in Nanjing accounted for 97 and 96 % of the city's total coal consumption, respectively, reflecting the highly centralized energy use of Nanjing.

Besides annual levels, monthly energy consumption, industrial production, and flue-gas concentrations from CEMS are obtained whenever possible through our plant-by-plant onsite investigations. The monthly distribution of emissions from key sources is then revised based on these data.

Emissions from on-road transportation are calculated using COPERT 4 (version 9.0) (EEA, 2012). The parameters required by the model, including vehicle population by type, fleet composition by control stage (Stage I–IV, equivalent to Euro I–IV), and annual average kilometers traveled (VKT), are taken from investigations by NJEPB. The detailed information for 2012 is summarized in Tables S1 and S2 in the Supplement. The traffic flows for the main roads in the city are compiled from the real-time observations of the Intelligent Traffic Violation Monitoring Systems (internal data of NJEPB). The spatial and diurnal distribution of emissions can then be quantified by combining the information of traffic flow and the road network.

For area sources including other small industry, solvent use, residential combustion, agricultural activity, and non-road transportation, emissions are estimated following previous work (Zhao et al., 2012a, b, 2013), with up-to-date emission factors from domestic measurements and city-scale activity levels. The energy consumption data are taken from the Environmental Statistics (internal data of NJEPB) and the agricultural and industrial outputs are mainly from the Nanjing Statistical Yearbook (NJNBS, 2013). Fire counts and intensity observed from MODIS (Moderate Resolution Imaging Spectroradiometer, https://earthdata.nasa.gov/data/near-real-time-data/firms) are used to determine the spatial and temporal distribution of emissions from biomass open burning. Regarding fugitive dust, information about individual construction sites in the city is obtained from NJEPB to improve the estimation of emission levels and spatial and temporal distributions. This includes location, period of operations, construction area, and amount of earthworks). The largest 221 construction sites in Nanjing in 2012

ACPD
15, 18691–18746, 2015

(accounting for 45 % of the total construction area) are shown in Fig. S1c in the Supplement.

2.2 Emission factors

As mentioned previously, parameters related to emission factors for key sources (CPP, CEM, ISP, and RCP) are obtained through onsite surveys for each plant. The parameters for CPP include boiler type, combustion technology, fuel quality (sulfur, ash, and volatile matter contents), types and pollutant removal efficiencies of APCDs (flue gas desulphurization (FGD), selective catalytic reduction (SCR)/selective non-catalytic reduction (SNCR), dust collection). Emission factors can then be determined or calculated based on the method described by Zhao et al. (2010). For cement production, the kiln type, PM removal efficiency of dust collectors, and fuel quality are investigated and emission factors are calculated following Lei et al. (2011) and Zhao et al. (2012a, 2013). For ISP, key parameters in four main processes (coking, sintering, pig iron production, and steelmaking) are obtained, including the SO_2 removal rate of FGD for sintering, PM removal rate of dust collectors, and the gas release ratios of coke ovens, blast furnaces, and basic oxygen furnaces. Emission factors for each process are then calculated following Zhao et al. (2012a, 2013). For the chemical industry, the surveyed parameters include the types and amounts of raw materials and products, the types and volumes of tanks, and technologies applied for VOC control. In particular, the emission factors for refineries are determined by industrial process, including production, storage, loading, and unloading (Wei et al., 2008; USEPA, 2002; EEA, 2013). Inter-annual variations in these parameters for major sources are tracked in the survey so that changing emission factors over time (2010–2012) can be determined. Table 1 summarizes the penetrations and removal efficiencies of APCDs for CPP and typical industries in Nanjing from 2010 to 2012. For other industrial sources, emission factors are taken mainly from the database by Zhao et al. (2011, 2013), after incorporating the most recent results from domestic measurements. Table S3 in the Supplement summarizes the emission factors for main industrial processes.

ACPD
15, 18691–18746, 2015

For other sources for which local emission factors are currently unavailable, emission factors are determined based on existing studies in other parts of China. If no domestic studies are available, recommendations of USEPA (2002) are applied. Road dust emissions are estimated following USEPA (2002), based mainly on the average weight of vehicles, silt loading of the road surface, and traffic flow. Those parameters are taken from Fan et al. (2007) and Huang et al. (2006), with some adjustments of road types for Nanjing. Emission factors of construction dust recommended by USEPA (2002) are used in this work, i.e., 0.026, 0.106, and 0.191 $(\mathrm{kg\,m^{-2}})\,\mathrm{month^{-1}}$ for $PM_{2.5}$, PM_{10}, and TSP, respectively. The mass fractions of BC and OC in construction $PM_{2.5}$ are assumed to be 2.4 and 3.4 %, respectively, from measurements by Zhao et al. (2009).

For gasoline stations, Nanjing completed installation of vapor recovery systems at all stations at the end of 2012. VOC emission factors for gas storage, loading, unloading and sales are determined at 0.03, 0.87, 0.10 and 2.44 $\mathrm{g\,kg^{-1}}$, respectively (Wei et al., 2008; Fu et al., 2013). Solvents include paints for buildings and furniture, ink, fabric coating adhesives, and pesticides. VOC emission factors for decorative adhesives, interior wall paints, and wood paints are taken from Fu et al. (2013), while those for other solvent use come mainly from Wei et al. (2008).

Emission factors for non-road transportation are mainly from Zhang et al. (2010) and Ye et al. (2014). Emission factors for household biofuel use are estimated based on results of various domestic measurements as summarized in Zhao et al. (2013) and Cui et al. (2015), while those for biomass open burning are from Li et al. (2007). NH_3 emissions from livestock farming and fertilizer use are taken from Dong et al. (2010), Yang (2008), and Yin et al. (2010).

ACPD
15, 18691–18746, 2015

3 Results

3.1 Inter-annual variability and sector distribution of emissions

The annual emissions of various air pollutants and CO_2 from anthropogenic sources in Nanjing are shown in Fig. 1a for 2010–2012. In 2010, the total emissions of SO_2, NO_x, CO, VOCs, NH_3, $PM_{2.5}$, PM_{10}, TSP, CO_2, BC and OC are estimated at 165, 216, 774, 224, 21, 71, 94, 158, 79 976, 6.2, and 6.7 Gigagrams (Gg), respectively. Note the numbers here for PM emissions do not include fugitive dust from construction and transportation, to facilitate comparison with inventories that omit the source. Despite large growth in coal consumption from 2010 to 2012, the emissions of SO_2 and NO_x in 2012 are estimated to be smaller than those in 2010, implying the effectiveness of emission control measures for the city in recent years. These measures include mainly the increased use of flue gas desulfurization (FGD) and selective catalytic reduction (SCR) systems in the power generation sector (see the detailed information in Table 1). The slight increase in SO_2 emissions between 2011 and 2012 resulted mainly from the growth in coal consumption in industries other than power generation, where FGD systems have not been widely deployed. PM emissions are estimated to be quite stable for the three years, with small increases in $PM_{2.5}$ and PM_{10}. Rising mass fractions of $PM_{2.5}$ to TSP (from 45 to 48 %) indicate the difficulty in controlling emissions of finer primary particles compared to coarser ones. For VOCs and NH_3, which have not been well regulated in national action plans for air pollution prevention and control (Zhao et al., 2014), the inter-annual variabilities of emissions are small and driven mainly by relative stability in chemical and agricultural production, respectively. While CO_2 continues to rise, no growth is estimated for CO from 2011 to 2012, implying improved overall combustion efficiency in the city.

Figure S2 in the Supplement shows the sector contributions to total emissions by year and species, as well as the shares of coal consumption by sector for comparison. From 2010 to 2012, power plants, iron and steel plants, and other industrial plants are the largest SO_2 sources, contributing 41–42, 14–19, and 32–23 % of total emissions,

ACPD
15, 18691–18746, 2015

respectively. NO_x emissions come mainly from power plants (45 %) and on-road transportation (20 %) throughout the time period. The shares of SO_2 and NO_x emissions from the power sector are clearly smaller than its shares of coal consumption (57–64 %) or CO_2 emissions (48–57 %), due largely to relatively stringent emission controls in the sector. Fugitive dust, particularly that of road origin, is identified as the dominant anthropogenic source of PM emissions. The fugitive dust shares of TSP are estimated to range 64–70 % during the research period, while smaller fractions are found for finer particles and carbonaceous aerosols. Apart from fugitive dust, iron and steel production plays a significant role in PM emissions in Nanjing, with its shares of TSP, PM_{10}, and $PM_{2.5}$ calculated at 15–16, 20–23, and 35–41 %, respectively. This results mainly from the large coal use by the sector, and relatively poor PM control measures of certain plants compared to other major coal-consuming sources, e.g., power plants. Iron and steel production is also identified as the biggest contributor of CO emissions for the city with its share reaching 60 % in 2012, even though emission factors for the sector in Nanjing (based on field investigations) are smaller than the national average (Zhao et al., 2012a). This is partly attributed to relatively little inefficient coal combustion at other sources in the city (e.g., in small industry and residential use), resulting in much lower fractions of CO emissions from those sources than the national averages. VOCs come mainly from chemical production (52 %) and solvent use (29–30 %). With vapor recovery systems increasingly applied, VOC emissions from gas stations decline during the research period. Despite an increase in vehicle population, the fractions of on-road transportation emissions for most species decrease from 2010 to 2012, attributed mainly to implementation of increasingly strict vehicle emission standards. From effective prohibition of burning of agricultural wastes, the emission contributions of this source, mainly of particles, carbonaceous aerosols, and CO, are also considerably reduced.

ACPD
15, 18691–18746, 2015

3.2 Spatial and temporal distribution

For simulation of atmospheric transport and chemistry, the emission inventories are allocated into a 3 km × 3 km grid system. For sources lacking specific location information, their emissions are assumed to be correlated with population density, with the exception of NH_3, which is allocated based on the density of agricultural GDP. Shown in Fig. 2 are the spatial distributions of SO_2, NO_x, $PM_{2.5}$ (exluding fugitive dust from construction and roads) and VOC emissions for Nanjing in 2012, and the locations of the ten largest point sources of each species. Relatively high emission densities are found in the urban area, particularly around certain large power generation and industrial sources. As illustrated Fig. 3, the fractions of emissions from point sources for all concerned species are estimated to exceed 50 %, as are those from the collective four key source types, with the exception of BC, at 38 %.

Monthly distributions of SO_2 emissions by sector and that of total emissions of all species for 2012 are respectively shown in Fig. S3a and b in the Supplement. Note again that fugitive dust from construction sites and roads is excluded. The results of MEIC are also provided in Fig. S3a for comparison. It can be seen that the temporal distributions of the two studies are similar except for residential emissions, which are smaller overall in this work compared to MEIC. As indicated by MODIS fire counts, over 90 % of biomass open burning occurred in May–July, leading to much higher OC emissions in those three months compared to any other time of the year. For other species, the temporal distributions of emissions correlate closely with those of activity levels, with a drop in February attributed mainly to reduced energy supply and industrial production during the Spring Festival. Pronounced diurnal variations of on-road transportation emissions are illustrated in Fig. S4 in the Supplement, with two peaks at the rush hours. The daily shares of CO and VOC emissions in the morning rush hour (16 %) are slightly higher than those of NO_x (14 %) and $PM_{2.5}$ (15 %). Based on the assumptions of COPERT, the cold start of most vehicles occurs in the morning, leading to larger CO and VOC emission factors during this time compared to those during

ACPD
15, 18691–18746, 2015

stable operation of vehicles. The influence of vehicle cold starts on emissions of NO_x and $PM_{2.5}$ is smaller.

3.3 Comparisons with other studies in emission estimates

Figure 1b compares our estimates of Nanjing emissions with those from other inventories (Fu et al., 2013; MEIC) for a common year, 2010. In the other studies, national or regional average levels for some parameters related to emissions, e.g., the penetrations and pollutant removal rates of emission control devices, are applied. These values can vary considerably from those based on plant-by-plant field investigations, leading to clear differences in emission estimates compared to the current work.

Our estimate of SO_2 emissions for Nanjing is 25 and 22 % higher than those of Fu et al. (2013) and MEIC, respectively, even though the plant-by-plant survey indicates an FGD penetration rate of 92 % of installed power generating capacity, higher than the provincial average of 85 % used in Fu et al. (2013). The higher estimate results because: (1) the total coal consumption from the Environmental Statistics applied in this work is 14 % larger than that provided by the Nanjing Almanac used in other studies (NJCLCC, 2011; see Sect. 4.6 for more discussion), and (2) a relatively lower removal efficiency of FGD is obtained from the onsite survey for 2010. Similar NO_x emission levels are found between current work and MEIC, while lower emissions were provided by Fu et al. (2013). According to filed survey, the penetration rate of SCR/SNCR increased from 44 to 67 %, and the NO_x removal efficiency increased from 18 to 77 % during 2010–2012 (Table 1). The penetration rate is much larger compared to the provincial average of 22 % applied in MEIC and Fu et al. (2013), partly offsetting a discrepancy in estimated emissions caused by larger activity levels used in current city-scale inventory.

Our estimates for $PM_{2.5}$, PM_{10}, and BC emissions (without fugitive dust emissions) are larger than those of Fu et al. (2013) or MEIC in 2010. This results mainly from larger emissions from industry (particularly iron and steel production), as the survey revealed that relatively old and inefficient wet dust collectors were still used at some

ACPD
15, 18691–18746, 2015

plants. OC emissions, however, are estimated to be lower than MEIC indicates, due mainly to very little coal or biomass burning in the city-level statistics.

VOC emissions estimated in this work in 2010 are 34 % larger than Fu et al. (2013) and 36 % larger than MEIC. In particular, emissions from refineries and chemical plants, calculated using detailed information on each plant's inputs of raw materials and the product types and amounts, are 116 % higher than those in regional inventories (Fu et al., 2013). Thus the fraction of total VOC emissions attributed to industrial processes is estimated at 48 % by us, larger than the YRD average level of 34 % (Fu et al., 2013). Given Nanjing is a city with large petroleum refining and chemical industries, and that much higher production of crude oil, gasoline, diesel and liquefied petroleum gas is reported than in other YRD cities in 2010 (NJNBS, 2013), the higher VOCs emissions indicated by the plant-based inventory is believed to better reflect the city's true industrial structure.

For CO, our estimates are 12 % higher for industry than those of MEIC, but 26 and 37 % lower respectively for residential and transportation sectors, resulting in 2 % lower emissions for anthropogenic sources as a whole. The discrepancy in sector contributions is caused mainly by the high percentage of centralized coal combustion in the city: power, iron and steel, cement, and chemical plants consumed over 95 % of the city's coal, based on our field survey. Our CO_2 emission estimate is 22 % higher than that of MEIC, resulting mainly from the difference in coal consumption reported by the Environmental Statistics database and the city almanac.

4 Assessment of the city-scale emission inventory

The current inventory is assessed to gauge improvements of emission estimates using a city-scale framework. The inter-annual variability, spatial distributions, and correlations of a number of species of the inventory are evaluated by comparison to available satellite and ground observations, and to downscaled national emission inventories.

ACPD
15, 18691–18746, 2015

4.1 Evaluation of inter-annual trends and spatial distribution of NO_x emissions with satellite observations

The inter-annual trend in NO_x emissions estimated bottom-up is compared with that of NO_2 vertical column densities (VCDs) based on satellite observations. The VCDs of tropospheric NO_2 are retrieved from the Ozone Monitoring Instrument (OMI) by the Royal Netherlands Meteorological Institute (Boersma et al., 2007, 2011), using monthly data with spatial resolution of $0.125^\circ \times 0.125^\circ$ (data source: http://www.temis.nl/airpollution/no2col/no2regioomimonth_v2.php). Illustrated in Fig. 4 are annual emissions estimated in this work for Nanjing from 2010 to 2012 and VCDs from 2005 to 2012 for 4 regions: Nanjing, Shanghai, 4 provinces in the YRD (including Jiangsu, Zhejiang, Anhui and Shanghai), and a rectangular region containing Nanjing (see Fig. S1a for reference). The first two represent NO_2 at city levels while the latter two represent regional levels. To eliminate seasonal variations, NO_2 VCDs are presented as 12 month moving averages, calculated as the means of the data for the previous and subsequent six months. All the data are normalized to the 2010 level of Nanjing. While NO_2 VCDs started declining around 2008 for Shanghai, it kept increasing for the rest of the YRD region including Nanjing until 2012. Clearly higher than the regional levels, the average NO_2 VCD for Nanjing approached that of Shanghai after 2010. This implies, on one hand, the benefits of Shanghai's strict emission controls of on-road vehicles and big power plants (K. Huang et al., 2014), implemented in advance of other regions. On the other hand, the growth of NO_2 for the rest of the YRD demonstrates the spread of air pollution source regions from major metropolitan areas to less developed cities nearby, and thereby suggests the need for increased efforts in emission and pollution abatement in those areas, as indicated by Zhang et al. (2012a). Decreased emissions in Nanjing are clearly indicated by this work after 2011, attributed mainly to the national policy of compulsory installation and running of SCR devices in the power sector. This inter-annual variation shows good consistency with that of OMI NO_2 VCD.

ACPD
15, 18691–18746, 2015

To further assess possible improvement of emission estimates by the current city-level inventory, the spatial distribution of monthly means of OMI NO_2 VCD in summer (June–August) 2010 over Nanjing is compared with that of two emission studies: (1) city-level emissions at spatial resolution of 3 km × 3 km by the current work, and (2) MEIC emissions developed at the provincial level with a resolution of 5 km × 5 km. For the purpose of visualization and further analysis, the emissions are reallocated to a 0.125° × 0.125° grid system from the original spatial distributions, consistent with the resolution of retrieved OMI NO_2 VCD. We assume that the NO_2 VCD from satellite observations reflect the anthropogenic NO_x emissions of the city for the following reasons. NO_x emissions in East China are predominantly anthropogenic (Mijling et al., 2013); lightning and soil sources as a share of total emissions are estimated to peak in July, when they account for 9 and 12 %, respectively (Lin et al., 2012). NO_x emissions in Nanjing are clearly larger than in surrounding areas (Huang et al., 2011), and the NO_2 VCD over the city is believed to be most influenced by local emissions.

As shown in Fig. 5, a similar spatial pattern of NO_x is captured by the gridded emissions and satellite observations, and relatively higher pollution in the urban area in the center of the city is indicated, attributed mainly to the combined effects of intensive transportation and large point sources. The emission inventories, however, underestimate the high-pollution areas compared to OMI observations, particularly MEIC. To further gauge improvement in spatial distribution by the city-scale emissions, correlations between the gridded emissions and the VCD are analyzed. As shown in Fig. 6a, the correlation coefficients (R) between the emissions and the VCDs are calculated at 0.450 and 0.408 for this work and MEIC, respectively, indicating better agreement by the city-scale inventory. Moreover, a sensitivity test on the correlation coefficients is conducted through step-wise exclusion of the grid cells with the largest emissions. Along with the increase in excluded grid cells, the R for this city-scale emission inventory remains above 0.43, while those of MEIC sharply decrease (Fig. 6b). In order to estimate emissions of the whole country, the MEIC is based mainly on energy and economic statistics at the provincial level, though it includes a limited number of major point

ACPD
15, 18691–18746, 2015

sources, e.g., power plants with relatively good documentation and large emissions. Emissions from other point sources are based on coarser inputs due to constraints of time, labor, and data availability. The current study, in contrast, compiled detailed information for all power plants and most other industrial sources in Nanjing through comprehensive survey investigation, as described in Sect. 2. Better estimates of emission levels and spatial distributions should thus be expected, particularly for small or medium-size emission sources. Once the grid cells dominated by major power plants are excluded from the two inventories, as shown in Fig. 6c, the current city-scale emissions still correlate well with satellite observations (R = 0.436) while MEIC shows little correlation (R = 0.085). The results reflect that inventories compiled at the provincial or regional level better estimate emissions of large sources than small or medium-sized ones, due to relative availability of information on power plants but much poorer nationwide data availability for other industrial plants. When focusing on smaller regions like cities, however, detailed information on more emission sources from onsite survey becomes crucial for improving emission estimates.

It should be noted that high NO_2 VCDs are found over the Yangtze River by OMI (roughly following the dark red zone in Fig. S5 in the Supplement) while current emission inventories cannot capture this. Possible underestimation of emissions from ships is indicated. Due to data limits, only ships arriving or leaving the port of Nanjing are taken into account in the current city-scale inventory, while those passing through Nanjing are omitted. Further investigation of the vessel flow along the Yangtze River is thus necessary to improve the estimation of ship emissions, which may be particularly influential at small spatial scales.

4.2 Spatial correlations between pollutant emissions and ambient concentrations from ground observations

Ambient concentrations for selected pollutants from ground observations are used to test the city-scale emission inventory. Daily averages of SO_2, NO_2, CO, and $PM_{2.5}$ concentrations for 2012 are obtained from the 9 state-operated monitoring stations

ACPD
15, 18691–18746, 2015

in Nanjing, mapped in Fig. S1d. The SO_2, NO_2, CO, and $PM_{2.5}$ concentrations were measured by Ecotech EC9850B, Ecotech EC9841B, Ecotech EC9830B and Met One 1020 analyzers, respectively. The emissions of specific pollutants around each site with a grid cell size of 0.04° × 0.04° are calculated from the 3 km × 3 km gridded inventories, and correlations with annual mean concentrations of corresponding species are analyzed. Since none of the city's key sources (CPP, CEM, ISP or RCP) are located in those grid cells, the effects of individual big sources on the correlation between emissions and observation are assumed to be limited.

As shown in Fig. 7a, modest agreement is found in spatial patterns between the observed concentrations and the emissions for SO_2 and NO_x (NO_2), with the R calculated at 0.58 and 0.46, respectively. SO_2 and NO_x have average atmospheric lifetimes of several days and one day, respectively, thus the ambient concentrations are expected to partly reflect emission intensities nearby and the correlation analysis adds support for the reliability of the city-scale emission inventory. As shown in Fig. 7b, the correlation coefficient for CO is calculated at 0.61, and it reaches 0.86 when the observation of the Caochangmen site is excluded, where extremely high emissions are calculated but low ambient levels were observed (to be further discussed in Sect. 4.4). Even with a longer lifetime (weeks to months) than SO_2 or NO_x, CO in the atmosphere over Nanjing results mainly from primary emissions from incomplete combustion, implying reasonable agreement between emissions and concentrations. However, emissions from small coal combustion sources still cannot be fully tracked or precisely quantified, and this evidence is thus tentative.

4.3 Evaluation of emissions against top-down constraints from observations

For certain pairs of pollutants that come from common sources and thus share emission characteristics, or weakly reactive species that are relatively stable in the atmosphere, correlations of ambient concentrations can provide useful "top-down" constraints on "bottom-up" estimates of primary emissions. In this work, the correlations of three pairs of species in the atmosphere – BC and CO, OC and EC, and CO_2 and CO

ACPD
15, 18691–18746, 2015

– are analyzed based on daily mean concentrations from ground observations in 2012. Combining the mass or molar ratios of emissions for corresponding species allows further evaluation of the city-scale inventory.

4.3.1 BC and CO

BC and CO both result from incomplete combustion of solid fuels and certain industrial processes such as coking. With relatively long atmospheric lifetime, CO is usually recognized as a tracer of pollution transport. Combined with BC levels, it can also be used to test emission inventories of the two species (most at regional or national scale), which is particularly useful for BC given its relatively large emission uncertainties (Kondo et al., 2011; Wang et al., 2011; Zhao et al., 2011, 2012a). We follow the method presented in Wang et al. (2011) but focus on evaluating the city-level, top-down emission ratio of BC to CO based on observations at Caochangmen in Nanjing (point A in Fig. S1d in the Supplement). We choose this site for emission evaluation for two main reasons. First, it is an urban site and thus assumed to be more representative for the city emissions, compared to suburban/rural sites that are more influenced by emissions from broader areas. Second, Caochangmen is the biggest and the most comprehensive state-operated station in the city. Among all the 9 state-operated sites in Nanjing, it is one and only station that conducts observation not only for the six criterion pollutants (i.e., SO_2, NO_2, CO, O_3, PM_{10}, and $PM_{2.5}$) but also for certain species including BC used here and CO_2 used later. Daily means of BC and CO concentrations are calculated based on the hourly data from continuous observations using Magee AE 31 and Ecotech EC9830B analyzers, respectively, and the correlation between the two species are then evaluated and used to check the bottom-up emission inventories. Since ambient levels of BC and CO depend not only on emissions but also on atmospheric processes (e.g., wet and dry depositions of BC, chemical reactions of CO with OH, and mixing of both BC and CO) that exert different influences on the two species (Wang et al., 2011), the top-down emission ratio of BC to CO ($BC/CO|_{E,top\text{-}down}$) is calculated from the observed BC/CO($dBC/dCO|_t$) by excluding the influence of the

ACPD
15, 18691–18746, 2015

above-mentioned atmospheric processes, as indicated in Eq. (2):

$$\mathrm{dBC/dCO}|_t = \mathrm{BC/CO}|_{\mathrm{E,top\text{-}down}} F_{\mathrm{dry}} F_{\mathrm{chem}} F_{\mathrm{mixing}} F_{\mathrm{wet}} \quad (2)$$

F_{wet} indicates the wet deposition screening. Based on precipitation data from the Weather Underground weather site (http://www.wunderground.com/history/), the data in precipitation days were excluded to eliminate the effects of wet deposition. F_{dry}, F_{chem} and F_{mixing} indicate the screening of dry deposition of BC, chemical reactions of CO with OH, and mixing of both BC and CO, respectively. Following the methods by Wang et al. (2011), F_{mixing} is set at 1 and $F_{\mathrm{chem+dry}}$ is calculated at 0.88 based on the lifetime of BC and CO in the atmosphere.

As shown in Fig. 8, the annual ratio of BC to CO from observations is estimated at 0.0071 $\mu g\,m^{-3}\,ppbv^{-1}$ by linear regression with the reduced major axis method (Hirsch and Gilroy, 1984), and it is 0.0073 $\mu g\,m^{-3}\,ppbv^{-1}$ if the days of wet deposition are excluded. Once influence from other atmospheric processes are further eliminated, $\mathrm{BC/CO}|_{\mathrm{E,top\text{-}down}}$ rises to 0.0084, lower than the ratio from the city-scale bottom-up emission inventory at 0.0097, or that from the MEIC national inventory at 0.0095. It should be noted that the downtown observation site is influenced heavily by local transportation, particularly gasoline vehicles that have relatively high CO but low BC emissions. Therefore, the top-down ratio of BC to CO observed at the site is expected to be somewhat lower than that of emissions over the entire city. The comparison of top-down and bottom-up results is thus roughly consistent with the city-scale emission inventory, although possible overestimation of BC, or underestimation of CO emissions are indicated.

Aside from mean annual levels, comparisons are also conducted for seasonal BC to CO ratios, as summarized in Table 2. The highest $\mathrm{BC/CO}|_{\mathrm{E,top\text{-}down}}$ is found in summer while the lowest is in winter. Such seasonal variation, however, is not indicated in the current bottom-up emission inventory, for the following possible reasons. First, as described in Sect. 2, the temporal distribution of emissions is based on investigation of large and medium enterprises. However, the species of concern here, especially BC,

ACPD
15, 18691–18746, 2015

come largely from small industrial and residential sources, for which temporal information is still lacking. For transportation, the increased cold start of vehicles in winter also leads to higher CO emissions that cannot be fully captured by COPERT (Cai and Xie, 2010; Xiao et al., 2004) and could thereby lead to an overestimate of BC/CO from the bottom-up method. Second, although Caochangmen is located in urban Nanjing, it would inevitably be influenced by emissions from wider regions outside the city that are not quantified in the city-scale inventory. For example, biomass burning, which has a higher BC to CO ratio than exists in the ambient atmosphere, occurs more frequently in less-developed areas such as northern Jiangsu and Anhui provinces than in Nanjing. According to MODIS, 79 % of agricultural fire points in Jiangsu 2012 were found in summer, elevating the ambient BC/CO in this season. Third, uncertainty exists about the estimation of F_{chem}. In winter, the lowest OH densities in the boundary layer resulting from the weakest radiation lead to the smallest CO sink, and the opposite is true in summer (Seiler et al., 1984; Huang et al., 2013). The elevated F_{chem} in summer should thus lead to reduced $BC/CO|_{E,top\text{-}down}$. In this work, however, the seasonal difference in F_{chem} cannot be precisely quantified precisely based on existing studies, and the same F_{chem} has to be used for all seasons, leading to possible overestimation of $BC/CO|_{E,top\text{-}down}$ for summer and underestimation for winter.

4.3.2 OC and EC

EC and primary OC result from incomplete combustion, and the ratio of OC to EC concentrations is used to evaluate carbonaceous aerosol emissions and the formation of secondary organic aerosols (SOA). From 2011 to 2013, ambient EC and OC in downwind Nanjing were collected using quartz filters and analyzed with a DRI Model 2001 Thermal/Optical Carbon Analyzer by season (Li et al., 2015). The ratios of primary OC to EC, $(OC/EC)_{pri}$, which are expected to exclude the effects of SOA and to serve as a top-down constraint of carbonaceous aerosol emissions, were determined by the lowest daily OC/EC observed during the sampling period for each season. The values of $(OC/EC)_{pri}$ were 1.70, 1.27, 1.53, and 1.85 for spring, summer, autumn, and winter,

ACPD
15, 18691–18746, 2015

respectively, with an annual average of 1.59. From the bottom-up estimates, the emission ratios of OC to BC in our city-scale emission inventory and MEIC are respectively 1.38 (for 2012) and 1.24 (for 2010, the most recent year for which MEIC emissions are available). Although our result is closer to observations and indicates improvement in emission estimation at the city level, the ratios of OC to BC emissions estimated bottom-up are clearly lower than the top-down $(OC/EC)_{pri}$ from observations. With few emission sources nearby, the observation site is thought to be less influenced by local sources (e.g., on-road transportation that has a relatively low emission OC to BC ratio) than the regional transport of pollutants (Li et al., 2015). Thus some sources with high OC to BC ratios that are uncommon in Nanjing but more dispersed outside the city contribute significantly to the observed concentrations at the site. Those sources include residential fossil and biomass combustion and biomass open burning. The OC to BC emission ratios of Jiangsu and Anhui provinces surrounding Nanjing are estimated respectively at 1.91 and 2.13 (Zhao et al., 2013), clearly larger than the local emission ratio of Nanjing. Moreover, the carbonaceous aerosol sampling procedure used by Li et al. (2015) would lead to positive artifacts of OC measurement and elevated OC to EC, since usage of quartz filters adsorbs some semivolatile organic compounds (SVOC) in the ambient atmosphere (Cheng et al., 2009). The uncertainty of OC quantification from this sampling approach can reach 100 % in some cities in China (Hu et al., 2008). Finally, uncertainty also exists in the $(OC/EC)_{pri}$ determination by Li et al. (2015), as the sample size from off-line measurements was small. To better evaluate city-level OC and BC emissions, therefore, more observational research with improved (e.g., long-term, continuous) measurements is strongly recommended at sites where local sources dominate.

4.3.3 CO_2 and CO

CO_2 is a well-known greenhouse gas, with the main anthropogenic sources fossil energy combustion and industrial processes. The ratios of CO_2 to CO emissions differ between source types, reflecting varying combustion efficiencies. The observed ratio

ACPD
15, 18691–18746, 2015

of CO_2 to CO levels in the atmosphere can thus be used as an indicator of energy efficiency, as well as a top-down test of emissions estimated bottom-up. The annual molar ratios of CO_2 to CO emissions in Nanjing are calculated at 65.7, 73.6, and 76.1 for 2010, 2011, and 2012, respectively, significantly higher than that in Beijing in 2008 (32.8, Zhao et al., 2012a). They are also higher than the mixing ratios observed in rural Beijing in 2008 (26.8, Y. Wang et al., 2010) or at Hatetuma Island (HAT), a remote site located off the coast of continental East Asia and influenced by air masses transported from East Asian countries from late fall to early spring (34.5, Tohjima et al., 2014). Given the large discrepancy, data from measurements in urban Nanjing (Caochangmen, Point A in Fig. S1d) are further analyzed to test the emissions. Daily mean concentrations of CO_2 and CO are derived from hourly observations using Thermo 410i and Ecotech EC9830B analyzers, respectively, for all of 2012. To exclude the effects of biogenic emissions that prevail in warm seasons, data for the winter months (January, February, and December) are used. The prevailing wind directions over Nanjing in winter are east and northeast, and large point sources, accounting for 64 % of the city's CO_2 emissions, are located to the east and northeast of Caochengmen, supporting use of the observational data for the current purpose.

The average observed concentrations of CO_2 and CO in winter were 421 ppmv and 608 ppbv, respectively. Based on the cumulative probability distribution of daily CO concentrations (as shown in Fig. S6 in the Supplement), the whole dataset is divided into three subsets: (1) below the 30th percentile (with average CO and CO_2 concentrations at 350 ppbv and 410 ppmv, respectively), (2) between the 30th and 95th percentile (677 ppbv for CO and 424 ppmv for CO_2), and (3) above the 95th percentile (above 1200 ppbv for CO and 448 ppmv for CO_2). We consider that subset (1) represents air masses from relatively clean areas outside Nanjing, and subset (2) a well-mixed blend of sources of CO_2 and CO over Nanjing. Subset (3) is assumed to indicate extremely serious regional pollution episodes, in which pollutants were trapped in a shallow inversion layer (Y. Wang et al., 2010). Subset (2) is believed to best reflect the typical effects of local emissions and is used for bottom-up emission comparisons.

ACPD
15, 18691–18746, 2015

Illustrated in Fig. 9 is the CO_2-CO correlation estimated with the reduced major axis method based on surface observations and the CO_2 to CO ratios from bottom-up emission inventories for Nanjing. Our estimate of the CO_2 to CO ratio (76.1) is closer to observations (86.9) than MEIC (52.8), implying improvement in the current city-scale inventory. The observed CO_2 to CO ratio, however, should theoretically be lower than that from emissions for the following three reasons. First, compared to CO, the observation of CO_2 at an urban site would be more influenced by sources within a broader region than the city, as CO_2 has a longer lifetime in the atmosphere. Thus it is not fully representative of the very centralized and large CO_2 emissions inside the city, particularly those from large point sources (e.g., 17 power plants and 2 iron and steel plants, which are estimated to account for 78 % of total CO_2 emissions in Nanjing), and the CO_2 to CO ratio from observations should be reduced. Second, the current emission inventory includes only the primary CO emissions while there may be a fair amount of secondary CO from the oxidation of NMVOC. Duncan et al. (2007) estimated that CO from NMVOC oxidation equaled nearly 50 % of global primary CO emissions. Given the intensive refineries and chemical plants and thereby elevated NMVOC emissions in Nanjing, considerable secondary CO from NMVOC oxidation can be expected, leading to a lower ratio of CO_2 to CO from observations than that from primary emissions. Third, as discussed previously, the Caochangmen site is influenced heavily by local transportation that exhibits a lower CO_2 to CO emission ratio than industry. We believe that the higher CO_2 to CO ratio from observations than bottom-up emissions reflect the uncertainties from both approaches. On one hand, emissions from certain species and sectors need to be further improved, e.g., CO from vehicles might be underestimated by the current work, since relatively poor management of vehicle emissions in China cannot be tracked by COPERT. On the other hand, we speculate that possible bias also exists in observations, with more discussion to follow in Sect. 4.4.

The larger molar ratios of CO_2 to CO in Nanjing than in Beijing, both from observations and emissions, are attributed mainly to the structure of emission sources. Nanjing is a city with intensive heavy industry, and over 90 % of coal was consumed by

ACPD
15, 18691–18746, 2015

power plants, iron and steel plants, cement plants, and large chemical enterprises with relatively high energy efficiencies, leading to elevated ratios of CO_2 to CO in emissions and thereby concentrations. Transportation, particularly gasoline vehicles, is additionally a significant emission source of CO compared to CO_2, and plays important roles in molar ratios of CO_2 to CO. For instance, Y. Wang et al. (2010) found significantly increased ambient CO_2/CO in September 2008 (46.4 ppmv ppmv^{-1}) compared to September 2005–2007 (23–29 ppmv ppmv^{-1}) in Beijing, resulting mainly from the temporary ban of vehicles for the Beijing Olympic Games and thereby decreased CO emissions. In 2012 the vehicle population in Beijing was 3.5 times that of Nanjing (NJNBS, 2013). Transportation was estimated to contribute 29–37 % of anthropogenic CO emissions in Beijing from various studies (MEIC; Zhao et al., 2013), but the value is much smaller in Nanjing (10 %), elevating the molar ratio of CO_2 to CO in the city.

4.4 Evaluation of local ground observations based on the city-scale emission inventory

While ground observations can be used as top-down constraints on emissions, we suggest that a high-resolution emission inventory can also be used to evaluate observational data. Although detailed local information demonstrably improves emission estimation, inconsistencies still exist between the city-scale emission inventory and ground observations of CO at Caochangmen. These inconsistencies include: (1) the significant increase in correlation coefficients between CO emissions and ambient concentrations at state-operated monitoring sites when the data at Caochangmen are excluded (from 0.61 to 0.86), as described in Sect. 4.2 and Fig. 7b, and (2) the higher CO_2/CO from observations at Caochangmen than that from city-scale emissions, which contradicts expectations based on atmospheric chemistry principles, as described in Sect. 4.3 and shown in Fig. 9. This suggests the possibility of instrumental or other error reflected in the relatively low CO concentrations observed at Caochengmen in 2012. Thus we conduct a comparison of CO concentrations between Caochangmen and another state-operated site, Shanxilu, for 2012 and 2014. Similar to Caochangmen, Shanxilu is also

ACPD
15, 18691–18746, 2015

an urban site, 3.5 km from Caochangmen. Frequency histograms of hourly CO concentrations at the two sites for 2012 and 2014 are shown in Fig. S7. It can be seen that CO levels at Caochangmen were significantly lower than those at Shanxilu in 2012 (Fig. S7a) but the CO levels were quite similar at the two sites in 2014 (Fig. S7b). Moreover, a clear difference (~ 30 %) in CO levels between 2012 and 2014 were found at Caochangmen (Fig. S7c) but not at Shanxilu (Fig. S7d). Given the very close distance and similar characteristics of the two sites, we tentatively assume that there should not be a significant difference in CO levels between them. Thus we conduct a sensitivity test by increasing the CO concentrations at Caochangmen by 30 % in 2012, and repeat the assessment of the city-scale emission inventory with the revised CO dataset. The correlation coefficient between CO emissions and ambient concentrations at the 9 state-operated sites would be increased substantially, from 0.62 to 0.83. The ratio of CO_2 to CO in winter from the revised observational data would decrease from to 86.9 to 66.8, close to and lower than the ratio from the bottom-up city-scale inventory (76.1), consistent with the expectation that observed CO_2/CO should be smaller than emissions. Such data revision is clearly speculative, but encourages further analysis when observational data for a longer period become available at both sites. The city-scale emission inventory may thus provide a basis to raise questions about the quality of local ground observations, which should not be taken for granted.

4.5 Comparison between city and national inventories for certain sources

To further explore the effects of methods and data employed in emission estimation at city and national levels, we conduct comparisons of emission levels and spatial distributions between the current inventory and MEIC for given pollutants from typical sources, including SO_2 from power generation, NO_x from transportation, and $PM_{2.5}$ from industry, for 2010 in Nanjing. Our estimates are reallocated to a resolution of 5 km × 5 km, the same as MEIC, so that spatial correlations between the two inventories can be quantified.

ACPD
15, 18691–18746, 2015

As shown in Fig. 10a, relatively good correlation in the spatial distributions of SO_2 emissions from power generation is found for the two inventories, with the R estimated at 0.74. The result indicates consistency between the emission estimates of the two studies for large point sources, as might be expected given their shared reliance on relatively transparent, publicly available information on power plants nationwide. Lacking detailed field investigation of individual sources, however, national inventory studies have to rely on standard information for which routine updates or revisions are not guaranteed, and the latest changes in individual plants, including the closure of small power units or relocation of some power plants, cannot be tracked fully or on a timely basis. This is reflected by a number of data points in Fig. 10a with positive emission values on one axis but zero on the other. Regarding the total emission levels, MEIC is 35 % lower than our estimate, attributed mainly to the different SO_2 removal efficiencies of FGD applied in the two studies. Based on the field measurement data that were reported by individual plants and verified by the local environmental protection bureau, the average removal efficiency of FGD for power plants in Nanjing in 2010 is estimated at 66 %, lower than the values commonly applied by researchers in national emission assessments (e.g., above 70 %, Zhao et al., 2013). The discrepancy reveals the value of site-specific investigation of key parameters influencing emission estimates, including the SO_2-removal rate of FGD.

For NO_x from transportation, the spatial R is calculated at 0.652 between the two estimates, and the value would rise to 0.75 if the two grid cells with the largest emissions in the city-scale inventory were excluded, as shown in Fig. 10b. Similar to the power sector, the general spatial pattern of emissions from transportation for the two inventories is largely consistent. The emissions in MEIC, however, are much more concentrated in downtown urban regions compared to our estimate, resulting from differences in spatial densities of population vs. transportation flows based on road networks. The former is commonly applied in spatial distribution of national emission inventories while the latter, when available through field investigation or real-time recording, are used in city-scale ones like ours. The total NO_x emissions from transportation estimated by

ACPD
15, 18691–18746, 2015

MEIC are 27 % lower than those by the city-scale inventory, suggesting introduction of considerable uncertainty when emissions estimated at the national level are downscaled to the city level based on proxies like population or economic activity.

In contrast to the above two cases, little correlation is found between the two estimates in the spatial distribution of $PM_{2.5}$ emissions from industrial sources (Fig. 10c). Shown in the maps of Fig. 10c are not only the $PM_{2.5}$ emissions but also the locations of the 20 largest emitting industrial enterprises. A clear discrepancy is observed between the distribution of those sources and emissions from MEIC, while much stronger consistency is found in the current work. Without sufficient information on individual sources, inventories developed at the national level tend to allocate large fractions of emissions into urban regions with relatively high densities of population and/or economic activity, assuming good spatial correlation between emissions and those proxies. Such correlation, however, likely weakens as pollution control in urban regions is implemented because it includes significant relocation of emission sources to suburban or rural areas (a primary element of urban pollution control policy in China). The total $PM_{2.5}$ emissions from industrial sources estimated by MEIC are 50 % lower than our estimate, moreover, because: (1) a national emission inventory based on the sector-average levels of controls and emission factors cannot capture atypical, extremely large sources (super emitters), and (2) coal consumption from the official statistics used by MEIC is much lower than the aggregate of individual sources evaluated in the field survey (3.0 vs. 5.0 million metric tons (Mt) for Nanjing, 2010). Comparisons and correlation analyses between inventories developed at different spatial scales, therefore, show the advantages of thorough investigation of individual emission sources, particularly for cities with many large industrial enterprises like Nanjing.

4.6 Uncertainty assessment of city-scale emission inventory

If probability distributions for each parameter of an emission inventory can be determined in advance, the uncertainties of the inventory can be quantified using Monte-Carlo simulation, as demonstrated and described in our previous studies (Zhao et al.,

ACPD
15, 18691–18746, 2015

2011, 2013). Targeting emissions at the city scale, the current work does not repeat the methods applied in those studies, as most information on the variation of emission factors obtained here is city- or device-dependent and cannot be simply applied generally. Instead, we try to identify some common sources of uncertainty in the development of city-level emission inventories, including: (1) the inconsistencies of activity-level data from various sources, and (2) the downscaling of activity data or emissions due to lack of city-level information.

There has been continuing concern about the accuracy and reliability of China's energy statistics for more than a decade (Sinton, 2001). Statistics from various sources report divergent energy consumption levels for the country, and the choice of activity-level data for emission inventories continues to be debated. For example, China's total energy use from national statistics has been inconsistent with that aggregated from provincial statistics, driving considerable differences in national emission estimates (Akimoto et al., 2006; Guan et al., 2012; Zhao et al., 2013). While Akimoto et al. (2006) concluded that an emission inventory based on province-by-province statistics were in better agreement with satellite observations, Guan et al. (2012) indicated that over-reporting in provincial energy statistics could be a factor. At the city level, however, there are far fewer evaluations of the accuracy of energy statistics. We find a clear discrepancy in energy consumption data in statistical sources for Nanjing: the total coal consumption in 2010 was reported at 27.9 Mt in the Nanjing Almanac (NJCLCC, 2011), while the value from the Environmental Statistics was 14 % higher, 31.9 Mt. The disparity results mainly from differences in data collection for small emission sources (enterprises). While data reporting systems and resulting data quality have been gradually improved for large- and medium-scale enterprises, many small-scale ones still do not maintain well-documented records on energy consumption, and the energy use of those enterprises is poorly captured by the city almanac (personal communications with officials from Nanjing Municipal Commission of Economy and Information Technology, 2014). Aimed at pollution control, the environmental statistical system obtains and verifies energy data for each enterprise through field surveys, and we thus believe that

ACPD
15, 18691–18746, 2015

these energy consumption data are more complete and reliable for emission inventory development. The uncertainty from such varied statistical sources could be reduced as retirement of small boilers and/or closure of small enterprises increases. Although the Nanjing Almanac stopped reporting coal consumption for the city after 2010, the Environmental Statistics indicates that the combined share of coal consumption by large- and medium-sized sources increased from 84 % in 2010 to 91 % in 2012, attributed to closure of small enterprises reporting highly uncertain energy data during the period.

Besides problems in the energy data, uncertainty in the city-scale emission inventory can also result from lack of information on certain industrial sectors in the city statistics. If field surveys of individual sources cannot be conducted due to labor or time constraints, emissions have to be estimated by downscaling national or provincial estimates. To evaluate the resulting uncertainty, air pollutant emissions from non-ferrous metal smelting and the production of brick and lime in Nanjing 2012 are recalculated by the downscaling provincial estimates method (method B). In this method, emissions in Jiangsu province are first calculated based on the provincial statistics and provincial average levels of emission control. Emissions in Nanjing are then obtained according to Nanjing's fraction of certain proxy (industrial GDP in this case) out of the whole province. The results are compared with those based on detailed source investigations (method A). Shown in Table 3 are the product output (activity level) and pollutant emissions estimated by methods A and B. The activity levels estimated from provincial-level information are much higher than the actual industrial production aggregated from individual plants, suggesting downscaling produces emission overestimates. For example, gaseous pollutant emissions calculated with method B are 2, 10, and 30 times larger than those produced by method A for brick, lime, and copper production, respectively. For PM emissions, the discrepancies in emissions between the two methods are smaller, attributed partly to the compensating effects of divergent removal efficiencies of dust collectors applied in the two methods, obtained either from plant-by-plant surveys (method A) or from national or provincial average levels (method B). The differences are believed to reflect disparities in the considerable fractions of total emis-

ACPD
15, 18691–18746, 2015

sions from OIN (i.e., industrial sources excluding iron and steel, cement, and chemical plants, for which information is relatively clear, as defined in Sect. 2.1), specifically 6, 22, 15, and 24 % of SO_2, NO_x, $PM_{2.5}$, and CO for lime production, as shown in Table 3. The results suggest relatively large uncertainties in city-level emission estimates lacking sufficient individual source information. In this case, moreover, the overestimates in Nanjing's emissions from downscaling provincial emissions would inevitably lead to underestimates for other cities within the province, weakening understanding of emission sources and the quantitative basis of regional control policies.

5 Policy implications

5.1 The effects of pollution control policies on emission abatement and air quality

Substantial efforts have been undertaken in specific Chinese sectors to achieve national targets in both energy conservation and emission reduction (Zhao et al., 2013). Under the air pollution control measures, clear benefits in emission abatement, particularly in the power and transportation sectors, are found for Nanjing from 2010 to 2012, a relatively short period. In the power sector, electricity generation increased by 58 % during 2010–2012 while that specifically from coal-fired plants grew by 47 %, reflecting the switch of coal to gas combustion and other diversification of power generation in the city. Meanwhile, coal consumption of the power sector increased by only 25 %, much slower than the resulting electricity generation, reflecting improved energy efficiency due to replacement of small and old power units with larger and more energy-efficient ones. As shown in Fig. S8a in the Supplement, the capacity share of large units (above 300 MW) increased from 72 % in 2010 to 78 % in 2012 while that of small ones (below 100 MW) decreased from 20 to 16 %. The penetration of large units raised as well the use of APCD for SO_2, NO_x, and PM, leading to significant reduction of emission factors by 30, 23, and 22 %, respectively. The decrease in emission factors can also be

ACPD
15, 18691–18746, 2015

seen for vehicles. With implementation of staged emission standards for new vehicles from 2010 to 2012, the emission factors of SO_2, NO_x, CO, and VOCs are estimated to have declined by 66, 33, 34, and 37 % for gasoline vehicles (Fig. S8b), those of NO_x, CO, and VOCs by 12, 13, and 24 % for diesel vehicles (Fig. S8c), and those of CO and VOCs by 25 and 34 % for motorcycles (Fig. S8d), respectively. The SO_2, CO, and VOCs emissions from on-road transportation decreased by 39, 11, and 27 %, respectively, while the vehicle population increased by 27 % in the city over the three years.

The benefits of emission control on air quality can be partly confirmed by comparisons of changes in emissions and ambient concentrations. During 16–24 August 2013 when the 2nd Asian Youth Games (AYG) were held in Nanjing, a series of extra emission controls measures were undertaken by the government to improve air quality for the Games. Those measures included increasing use of low-sulfur coal at power plants, closing small factories with relatively large pollutant emissions, stopping construction in some regions, and restricting traffic. Taking these extra measures into account, the emissions of SO_2, NO_x, $PM_{2.5}$, PM_{10}, and CO over 16–24 August 2013 are estimated to have declined 23, 31, 21, 14, and 33 %, respectively, compared to those in the same period in 2012, based on the monthly distributions described in Sect. 3.2 (see Table S4 in the Supplement). Correspondingly, the daily average concentrations for those pollutants in Nanjing during the AYG period were found to decline by 22, 27, 10, 5, and 22 %, respectively, compared to the same period in 2012 (Yu et al., 2014). Although changes in other factors including meteorological conditions also influenced air quality, the consistency between the reduced emissions and concentrations suggests that local emission abatement played a primary role in the air quality improvement.

5.2 Effects of super emitters and small sources on emission levels and spatial distributions

For cities with intensive, heavily polluting industries like Nanjing, large point sources with significant energy consumption and/or industrial production are estimated to dom-

ACPD
15, 18691–18746, 2015

inate the levels and spatial distribution of emissions of the city. As shown in Fig. 3, the areas with high emission densities in Nanjing are in good agreement with geographical locations of point sources for all pollutants. The ten largest point sources of SO_2 emissions are estimated to account for 54 % of total emissions in the city (Fig. 2a), and the analogous number for NO_x is 43 % (Fig. 2b). For $PM_{2.5}$, as shown in Fig. 2c, the ten largest sources are estimated to be responsible for 75 % of total primary emissions in Nanjing (excluding construction and road dust). In particular, extremely high emissions are found for iron and steel plants, resulting mainly from the high production of steel and reliance on wet scrubbers with relatively low removal efficiencies (annual average of 85 %) in the exhaust streams of basic oxygen furnaces. Similarly, the ten largest refineries and chemical plants shown in Fig. 2d are responsible for 52 % of VOC emissions in Nanjing. The dominant roles of these big sources on emission levels and spatial distributions indicate that careful investigation and analysis of source-specific parameters relevant to emissions from these super emitters (e.g., removal efficiency of APCDs) are particularly crucial to the reliability of city-scale emission inventories.

Although large point sources dominate emissions at the city level, the contributions from scattered small sources cannot be overlooked. As shown in Fig. 3, the fractions of air pollutant emissions from power, cement, iron and steel, and chemical plants to the city's total emissions are estimated to range from 38 to 88 %, significantly lower than that of coal consumption (96 %). Despite the tiny share of coal use, decentralized small coal combustion sources have a relatively high proportion of emissions, resulting from poorer emission control technologies and management than big enterprises. Regarding emission abatement and air quality improvement, it is imperative to expand pollution control from large sources to small- and medium-sized enterprises, as the potential for further reductions from the major sources are diminishing due to near-saturation of APCDs. As for improvement of emission inventories, more varied and uncertain emission factors for small boilers and kilns result from much greater diversities of manufacturing technologies. This necessitates more field measurements

ACPD
15, 18691–18746, 2015

in the future to inform the application of emission factors in inventories and to better understand the emission characteristics of small sources.

6 Conclusions

With updated methods and substantial new data on local emission sources, a city-scale emission inventory of air pollutants and CO_2 is developed for Nanjing for three years, 2010–2012. Through plant-by-plant onsite surveys, emission factors, spatial and temporal emission distributions, and estimates of total emissions for major sources (power, cement, iron and steel, and refineries and chemical plants) are especially improved. Emissions in the city are dominated by large point sources, or super emitters. Despite large increases in energy consumption and industrial production, the emissions of most concerned pollutants were largely stable during the period, particularly SO_2 and NO_x, attributed to increased use and air pollutant removal rates of APCDs under national policies of air pollution control. The current estimates are consistent with the inter-annual variability of NO_2 VCD observed from OMI. The improvement of emission estimates by city-scale assessment is further indicated by analyses of spatial correlations with observations by satellite (for NO_x) and ground stations (for SO_2, NO_x, and CO), as well as by top-down constraints (BC/CO, OC/EC, and CO_2/CO) provided by ground-based observations. Analyses of bottom-up emission inventories, moreover, can identify possible errors in observational datasets, encouraging further investigation.

Limitations remain in the current work. First, some available and potentially valuable information cannot yet be fully exploited to improve emission estimates. CEMS data help to determine the time distribution of emissions, for example, but are currently less useful for estimating absolute emission levels, due to incompleteness and systematic errors in relevant parameters (e.g., flue gas flow rate). Second, since emission factors for some sources are still based on provincial or national assessments due to lack of local information, the uncertainties of the city-scale emission inventory have not yet

ACPD
15, 18691–18746, 2015

been systematically quantified. In particular, the degree of uncertainty in the city-scale inventory compared to that of national ones remains unknown. Finally, it is currently difficult to assess emissions of some species believed to have high emission uncertainty, e.g., VOC and NH_3, due to lack of sufficient instrumental observations. More field measurements of both emissions and ambient levels of these species are thus recommended in the future.

The Supplement related to this article is available online at doi:10.5194/acpd-15-18691-2015-supplement.

Acknowledgements. This work was sponsored by the Natural Science Foundation of China (41 205 110), Natural Science Foundation of Jiangsu (BK20140020 and BK2012310), Ministry of Science and Technology of China (2011BAK21B00), and Collaborative Innovation Center for Regional Environmental Quality. We would like to thank Hongxin Bao and Danning Zhang from NJEPB for technical support of this work, and TEMIS for free use of their monitoring data. The contents of this paper are solely the responsibility of the authors and do not necessarily represent the official views of the sponsors.

References

Akimotoa, H., Oharaa, T., Kurokawac, J. I., and Horii, N.: Verification of energy consumption in China during 1996–2003 by using satellite observational data, Atmos. Environ., 40, 7663–7667, 2006.

Boersma, K. F., Eskes, H. J., Veefkind, J. P., Brinksma, E. J., van der A, R. J., Sneep, M., van den Oord, G. H. J., Levelt, P. F., Stammes, P., Gleason, J. F., and Bucsela, E. J.: Near-real time retrieval of tropospheric NO_2 from OMI, Atmos. Chem. Phys., 7, 2103–2118, doi:10.5194/acp-7-2103-2007, 2007.

Boersma, K. F., Eskes, H. J., Dirksen, R. J., van der A, R. J., Veefkind, J. P., Stammes, P., Huijnen, V., Kleipool, Q. L., Sneep, M., Claas, J., Leitão, J., Richter, A., Zhou, Y., and Brun-

ACPD
15, 18691–18746, 2015

ner, D.: An improved tropospheric NO_2 column retrieval algorithm for the Ozone Monitoring Instrument, Atmos. Meas. Tech., 4, 1905–1928, doi:10.5194/amt-4-1905-2011, 2011.
Cai, H. and Xie, S. D.: Determination of emission factors from motor vehicles under different emission standards in China, Acta Scientiarum Naturalium Universitatis Pekinensis, 3, 319–326, 2010 (in Chinese).
Cheng, Y., He, K. B., Duan, F. K., Zheng, M., Ma, Y. L., and Tan, J. H.: Measurement of semivolatile carbonaceous aerosols and its implications: a review, Environ. Int., 35, 674–681, 2009.
Cui, H., Mao, P., Zhao, Y., Nielsen, C. P., and Zhang, J.: Patterns in atmospheric carbonaceous aerosols in China: emission estimates and observed concentrations, Atmos. Chem. Phys. Discuss., 15, 8983–9032, doi:10.5194/acpd-15-8983-2015, 2015.
Dong, W. X., Xing, J., and Wang, S. X.: Temporal and spatial distribution of anthropogenic ammonia emissions in China, Environ. Sci., 31, 1457–1463, 2010 (in Chinese).
Duncan, B. N., Logan, J. A., Bey, I., Megretskaia, I. A., Yantosca, R. M., Novelli, P. C., Jones, N. B., and Rinsland, C. P.: Global budget of CO, 1988–1997: source estimates and validation with a global model, J. Geophys. Res., 112, D22301, doi:10.1029/2007JD008459, 2007.
European Environment Agency (EEA): COPERT 4-Computer Programme to Calculate Emissions from Road Transport, User Manual (Version 9.0), Copenhagen, Denmark, 2012.
European Environment Agency (EEA): EMEP/CORINAIR Emission Inventory Guidebook-2013, available at: http://www.eea.europa.eu//publications/emep-eea-guidebook-2013 (last access: 07 July 2015), 2013.
Fan, S. B., Tian, G., Li, G., and Shao, X.: Emission characteristics of paved roads fugitive dust in Beijing, Environ. Sci., 28, 2396–2399, 2007 (in Chinese).
Fu, X., Wang, S., Zhao, B., Xing, J., Cheng, Z., Liu, H., and Hao, J.: Emission inventory of primary pollutants and chemical speciation in 2010 for the Yangtze River Delta region, China, Atmos. Environ., 70, 39–50, 2013.
Guan, D., Liu, Z., Geng, Y., Lindner, S., and Hubacek, K.: The gigatonne gap in China's carbon, Nat. Clim. Change, 2, 672–675, 2012.
Hirsch, R. M. and E. J. Gilroy.: Methods of fitting a straight-line to data-Examples in water resources, Water Resour. Bull., 20, 705–711, 1984.

ACPD
15, 18691–18746, 2015

Hu, M., Deng, Z., Wang, Y., Lin, P., Zeng, L., Kondo, Y., and Zhao, Y.: Comparison of EC/OC in $PM_{2.5}$ between filter sampling off-line analysis and in situ on-line measurement, Environ. Sci., 29, 3297–3303, 2008 (in Chinese).
Hua, L., Guo, J., Xu, Z. Y., Hu, Y. Q., Huang, Y., and Zou, B. D: Analysis of PM_{10} source profiles in Beijing, Environ. Monit. China, 22, 64–71, 2006 (in Chinese).
Huang, C., Chen, C. H., Li, L., Cheng, Z., Wang, H. L., Huang, H. Y., Streets, D. G., Wang, Y. J., Zhang, G. F., and Chen, Y. R.: Emission inventory of anthropogenic air pollutants and VOC species in the Yangtze River Delta region, China, Atmos. Chem. Phys., 11, 4105–4120, doi:10.5194/acp-11-4105-2011, 2011.
Huang, K., Fu, J. S., Gao, Y., Dong, X, Y., Zhuang, G. S., and Lin, Y. F.: Role of sectoral and multi-pollutant emission control strategies in improving atmospheric visibility in the Yangtze River Delta, China, Environ. Pollut., 184, 426–434, 2014.
Huang, R. J., Zhang, Y., Bozzetti, C., Ho, K. F., Cao, J. J., Han, Y., Daellenbach, K. R., Slowik, J. G., Platt, S. M., Canonaco, F., Zotter, P., Wolf, R., Pieber, S. M., Bruns, E. A., Crippa, M., Ciarelli, G., Piazzalunga, A., Schwikowski, M., Abbaszade, G., Schnelle-Kreis, J., Zimmermann, R., An, Z., Szidat, S., Baltensperger, U., Haddad, I. E., and Prevot, A. S.: High secondary aerosol contribution to particulate pollution during haze events in China, Nature, 514, 218–222, 2014.
Huang, X., Huang, X. X., Wang, T. J., Zhuang, B. L., Li, S., Xie, M., Han, Y., Yang, X. Q., Sun, J. N., Ding, A. J., and Fu, Z. B.: Observation and analysis of urban upper atmospheric carbon monoxide in Nanjing, China Environ. Sci., 33, 1577–1584, 2013.
Huang, Y. M.: Study on the Emission Estimation and Spatial Distribution of Urban Fugitive Dust, M.Sc. thesis, East China Normal University, Shanghai, 2006 (in Chinese).
Kim, S.-W., Heckel, A., Frost, G. J., Richter, A., Gleason, J., Burrows, J. P., McKeen, S., Hsie, E.-Y., Granier, C., and Trainer, M.: NO_2 columns in the western United States observed from space and simulated by a regional chemistry model and their implications for NO_x emissions, J. Geophys. Res., 114, D11301, doi:10.1029/2008JD011343, 2009.
Kondo, Y., Oshima, N., Kajino, M., Mikami, R., Motcki, N., Takegawa, N., Verma, R. L., Kajii, Y., Kato, S., and Takami, A.: Emissions of black carbon in East Asia estimated from observations at a remote site in the East China Sea, J. Geophys. Res., 116, D16201, doi:10.1029/2011JD015637, 2011.
Kurokawa, J., Ohara, T., Morikawa, T., Hanayama, S., Janssens-Maenhout, G., Fukui, T., Kawashima, K., and Akimoto, H.: Emissions of air pollutants and greenhouse gases over

ACPD
15, 18691–18746, 2015

Asian regions during 2000–2008: Regional Emission inventory in ASia (REAS) version 2, Atmos. Chem. Phys., 13, 11019–11058, doi:10.5194/acp-13-11019-2013, 2013.
Lei, Y., Zhang, Q., Nielsen, C. P., and He, K. B.: An inventory of primary air pollutants and CO_2 emissions from cement industry in China, 1990–2020, Atmos. Environ., 45, 147–154, 2011.
Li, B., Zhang, J., Zhao, Y., Yuan, S. Y., Zhao, Q. Y., Shen. G. F., and Wu, H. S.: Seasonal variation of urban carbonaceous aerosols in a typical city Nanjing in Yangtze River Delta, China, Atmos. Environ., 106, 223–231, 2015.
Li, X. H., Wang, S. X., Duan, L., Hao, J. M, Li, C., Chen, Y. S., and Yang, L.: Particulate and trace gas emissions from open burning of wheat straw and corn stover in China, Environ. Sci. Technol., 41, 6052–6058, 2007.
Lin, J.-T.: Satellite constraint for emissions of nitrogen oxides from anthropogenic, lightning and soil sources over East China on a high-resolution grid, Atmos. Chem. Phys., 12, 2881–2898, doi:10.5194/acp-12-2881-2012, 2012.
Mijling, B., van der A, R. J., and Zhang, Q.: Regional nitrogen oxides emission trends in East Asia observed from space, Atmos. Chem. Phys., 13, 12003–12012, doi:10.5194/acp-13-12003-2013, 2013.
Nanjing Bureau of Statistics (NJNBS): Statistical Yearbook of Nanjing, China Statistics Press, Beijing, 2013 (in Chinese).
Nanjing Committee of Local Chronicles Compilation (NJCLCC): Nanjing Almanac, Editorial Department of Nanjing Almanac, Nanjing, 2011.
National Bureau of Statistics of China (NBSC): China Statistical Yearbook, China Statistics Press, Beijing, 2013 (in Chinese).
Ohara, T., Akimoto, H., Kurokawa, J., Horii, N., Yamaji, K., Yan, X., and Hayasaka, T.: An Asian emission inventory of anthropogenic emission sources for the period 1980–2020, Atmos. Chem. Phys., 7, 4419–4444, doi:10.5194/acp-7-4419-2007, 2007.
Seiler, W., Giehl, H., Brunke, E. G., and Halliday, E.: The seasonality of CO abundance in the Southern Hemisphere, Tellus B, 36, 219–231, 1984.
Sinton, J. E.: Accuracy and reliability of China's energy statistics, China Econ. Rev., 12, 373–383, 2001.
Streets, D. G., Bond, T. C., Carmichael, G. R., Fernandes, S. D., Fu, Q., He, D., Klimont, Z., Nelson, S. M., Tsai, N. Y., Wang, M. Q., Woo, J.-H., and Yarber, K. F.: An inventory of gaseous and primary aerosol emissions in Asia in the year 2000, J. Geophys. Res., 108, 8809, 2003.

ACPD
15, 18691–18746, 2015

Timmermans, R. M. A., Denier van der Gon, H. A. C., Kuenen, J. J. P., Segers, A. J., Honoré, C., Perrussel, O., Builtjes, P. J. H., and Schaap, M.: Quantification of the urban air pollution increment and its dependency on the use of down-scaled and bottom-up city emission inventories, Urban Climate, 6, 44–62, 2013.

Tohjima, Y., Kubo, M., Minejima, C., Mukai, H., Tanimoto, H., Ganshin, A., Maksyutov, S., Katsumata, K., Machida, T., and Kita, K.: Temporal changes in the emissions of CH_4 and CO from China estimated from CH_4/CO_2 and CO/CO_2 correlations observed at Hateruma Island, Atmos. Chem. Phys., 14, 1663–1677, doi:10.5194/acp-14-1663-2014, 2014.

U.S. Environmental Protection Agency (USEPA): Compilation of Air Pollutant Emission Factors (AP-42), 5th edn., available at: http://www.epa.gov/ttnchie1/ap42/ (last access: 07 July 2015), 2002.

Wang, L., Zhang, P., Tan, S., Zhao, X., Cheng, D., Wei, W., Su, J., and Pan, X.: Assessment of urban air quality in China using air pollution indices (APIs), JAPCA J. Air Waste Ma., 63, 170–178, 2013.

Wang, L. T., Wei, Z., Yang, J., Zhang, Y., Zhang, F. F., Su, J., Meng, C. C., and Zhang, Q.: The 2013 severe haze over southern Hebei, China: model evaluation, source apportionment, and policy implications, Atmos. Chem. Phys., 14, 3151–3173, doi:10.5194/acp-14-3151-2014, 2014.

Wang, S., Zhao, M., Xing, J., Wu, Y., Zhou, Y., Lei, Y., He, K., Fu, L., Hao, J.: Quantifying the air pollutants emission reduction during the 2008 Olympic Games in Beijing, Environ. Sci. Technol., 44, 2490–2496, 2010.

Wang, Y., Munger, J. W., Xu, S., McElroy, M. B., Hao, J., Nielsen, C. P., and Ma, H.: CO_2 and its correlation with CO at a rural site near Beijing: implications for combustion efficiency in China, Atmos. Chem. Phys., 10, 8881–8897, doi:10.5194/acp-10-8881-2010, 2010.

Wang, Y. X., Wang, X., Kondo, Y., Kajino, M., Munger, J. W., and Hao, J. M.: Black carbon and its correlation with trace gases at a rural site in Beijing: top-down constraints from ambient measurements on bottom-up emissions, J. Geophys. Res., 116, D24304, doi:10.1029/2011JD016575, 2011.

Wei, W., Wang, S. X., Chatani, S., Klimont, Z., Cofala, J., and Hao, J. M.: Emission and speciation of non-methane volatile organic compounds from anthropogenic sources in China, Atmos. Environ., 42, 4976–4988, 2008.

ACPD
15, 18691–18746, 2015

Xiao, J. H., Ma, W., Wang, J. X., and Wang, X. W.: A simulation of cold start emission characteristics of gasoline engine with Euro-III cycle on engine test bench, Automot. Eng., 6, 639–647, 2004 (in Chinese).
Yang, Z. P.: Estimation of Ammonia Emission From Livestock in China Based on Mass-Flow Method and Regional Comparison, M.Sc. thesis, Peking University, Beijing, 2008 (in Chinese).
Ye, S. Q., Zheng, J. Y., Pan, Y. Y., Wang, S. S., Lu, Q., and Zhong, L. J.: Marine emission inventory and its temporal and spatial characteristics in Guangdong Province, Acta Sci. Circum., 34, 537–547, 2014 (in Chinese).
Yin, S. S., Zheng, J. Y., Zhang, L. J., and Zhong, L. J.: Anthropogenic ammonia emission inventory and characteristic in the Pearl River Delta region, Environ. Sci., 31, 1146–1151, 2010 (in Chinese).
Yu, Y. Y., Xie, F. J., Lu, X. B., Zhu, Z. F., and Shu, Y.: The environmental air quality condition and the reason analysis during the Asian Youth Games of Nanjing, Environ. Monit. Forewarning, 6, 5–17, 2014 (in Chinese).
Zhang, L. J., Zheng, J. Y., Yin, S. S., Peng, K., and Zhong, L. J.: Development of non-road mobile source emission inventory for the Pearl River Delta region, Environ. Sci., 31, 886–891, 2010 (in Chinese).
Zhang, Q., Streets, D. G., Carmichael, G. R., He, K. B., Huo, H., Kannari, A., Klimont, Z., Park, I. S., Reddy, S., Fu, J. S., Chen, D., Duan, L., Lei, Y., Wang, L. T., and Yao, Z. L.: Asian emissions in 2006 for the NASA INTEX-B mission, Atmos. Chem. Phys., 9, 5131–5153, doi:10.5194/acp-9-5131-2009, 2009.
Zhang, Q., Geng, G. N., Wang, S. W., Richter, A., and He, K. B.: Satellite remote sensing of changes in NOx emissions over China during 1996–2010, Chinese Sci. Bull., 57, 2857–2864, 2012a.
Zhang, Q., He, K., and Huo, H.: Cleaning China's air, Nature, 484, 161–162, 2012b.
Zhao, P. S., Feng, Y. C., Jin, J., Han, B., Bi, X. H., Zhu, T., and Zhang, X. L.: Characteristics and control indicators of fugitive dust from building construction sites, Acta Science Circumstantiae, 29, 1618–1623, 2009 (in Chinese).
Zhao, Y., Wang, S. X., Duan, L., Lei, Y., Cao, P. F., and Hao, J. M.: Primary air pollutant emissions of coal-fired power plants in China: current status and future prediction, Atmos. Environ., 42, 8442–8452, 2008.

ACPD
15, 18691–18746, 2015

Zhao, Y., Wang, S. X., Nielsen, C. P., Li, X. H., and Hao, J. M.: Establishment of a database of emission factors for atmospheric pollutants from Chinese coal-fired power plants, Atmos. Environ., 44, 1515–1523, 2010.

Zhao, Y., Nielsen, C. P., Lei, Y., McElroy, M. B., and Hao, J.: Quantifying the uncertainties of a bottom-up emission inventory of anthropogenic atmospheric pollutants in China, Atmos. Chem. Phys., 11, 2295–2308, doi:10.5194/acp-11-2295-2011, 2011.

Zhao, Y., Nielsen, C. P., McElroy, M. B., Zhang, L., and Zhang, J.: CO emissions in China: uncertainties and implications of improved energy efficiency and emission control, Atmos. Environ., 49, 103–113, 2012a.

Zhao, Y., Nielsen, C. P., and McElroy, M. B.: China's CO_2 emissions estimated from the bottom up: recent trends, spatial distributions, and quantification of uncertainties, Atmos. Environ., 59, 214–223, 2012b.

Zhao, Y., Zhang, J., and Nielsen, C. P.: The effects of recent control policies on trends in emissions of anthropogenic atmospheric pollutants and CO_2 in China, Atmos. Chem. Phys., 13, 487–508, doi:10.5194/acp-13-487-2013, 2013.

Zhao, Y., Zhang, J., and Nielsen, C. P.: The effects of energy paths and emission controls and standards on future trends in China's emissions of primary air pollutants, Atmos. Chem. Phys., 14, 8849–8868, doi:10.5194/acp-14-8849-2014, 2014.

Zheng, B., Huo, H., Zhang, Q., Yao, Z. L., Wang, X. T., Yang, X. F., Liu, H., and He, K. B.: High-resolution mapping of vehicle emissions in China in 2008, Atmos. Chem. Phys., 14, 9787–9805, doi:10.5194/acp-14-9787-2014, 2014.

Zheng, J., Zhang, L., Che, W., Zheng, Z., and Yin, S.: A highly resolved temporal and spatial air pollutant emission inventory for the Pearl River Delta region, China and its uncertainty assessment, Atmos. Environ., 43, 5112–5122, 2009.

ACPD
15, 18691–18746, 2015

Table 1. The capacity penetrations, average removal efficiencies of APCDs, and flue gas release ratios for key sources in Nanjing.

	CPP-FGD Penetration	SO_2 removal efficiency	CPP-SCR/SNCR Penetration	NO_x removal efficiency	CEM-dust collector[a] TSP removal efficiency
2010	92.4 %	66.0 %	43.7 %	17.7 %	96.9 %
2011	97.0 %	78.5 %	66.6 %	41.8 %	97.0 %
2012	98.3 %	81.2 %	67.4 %	77.0 %	99.6 %
	ISP coke oven Gas release ratio	ISP blast furnace Gas release ratio	ISP sintering-FGD SO_2 removal efficiency	ISP pig iron production-fabric filter TSP removal efficiency	ISP steelmaking-dust collector[b] TSP removal efficiency
2010	0.5 %	1.5 %	70.0 %	98.9 %	97.3 %
2011	0.5 %	1.5 %	70.0 %	98.9 %	96.7 %
2012	0.5 %	1.5 %	70.0 %	98.8 %	96.7 %

[a] Including the fabric filter and the electrostatic precipitator.
[b] Including the fabric filter and the wet scrubber.

ACPD
15, 18691–18746, 2015

Table 2. The average concentrations of BC and CO and correlation of BC to CO from observations at Caochangmen and the ratios of bottom-up BC to CO emissions by season in Nanjing, 2012.

	Urban observation							Bottom-up inventory
	Avg. BC[a] ($\mu g\,m^{-3}$)	Avg. CO[a] (ppbv)	Avg. BC[b] ($\mu g\,m^{-3}$)	Avg. CO[b] (ppbv)	BC/CO[a] ($\mu g\,m^{-3}\,ppbv^{-1}$)	BC/CO[b] ($\mu g\,m^{-3}\,ppbv^{-1}$)	$BC/CO_{E,top\text{-}down}$[c] ($\mu g\,m^{-3}\,ppbv^{-1}$)	$BC/CO_{E,bottom\text{-}up}$ ($\mu g\,m^{-3}\,ppbv^{-1}$)
Spring	2.946	661.3	3.009	684.9	0.0070	0.0072	0.0082	0.0101
Summer	2.644	490.3	3.000	491.0	0.0083	0.0085	0.0097	0.0096
Autumn	4.206	619.6	3.822	627.1	0.0081	0.0081	0.0092	0.0095
Winter	3.007	615.0	3.068	637.7	0.0051	0.0060	0.0068	0.0096
Overall	3.156	588.0	3.264	600.5	0.0071	0.0074	0.0084	0.0097

[a] All the observation data included.
[b] The influence of wet deposition excluded.
[c] The influence of wet and dry deposition, chemical reactions with OH radicals, and mixing excluded.

ACPD
15, 18691–18746, 2015

Table 3. Comparisons of emission estimations using method A (plant-by-plant survey) and B (downscaling from provincial levels) for brick, lime, and copper production in Nanjing, 2012.

	Production[a]		SO_2 emissions		NO_x emissions		$PM_{2.5}$ emissions		CO emissions	
	Method A	Method B	B/A	(B-A)/OIN[b]	B/A	(B-A)/OIN	B/A	(B-A)/OIN	B/A	(B-A)/OIN
Brick	14	29			2.0	10 %	2.0	19 %	2.0	13 %
Lime	207	2050	9.9	6 %	9.9	22 %	3.6	15 %	9.9	24 %
Copper	1.3	39	31.1	24 %			3.6	13 %		

[a] The units are 10^9 bricks, 10^3 t-lime and 10^3 t-copper, respectively.
[b] Recall from Sect. 2.1 that OIN indicates emissions from other industry (iron and steel, cement production and chemical industry excluded) estimated at city level.

ACPD
15, 18691–18746, 2015

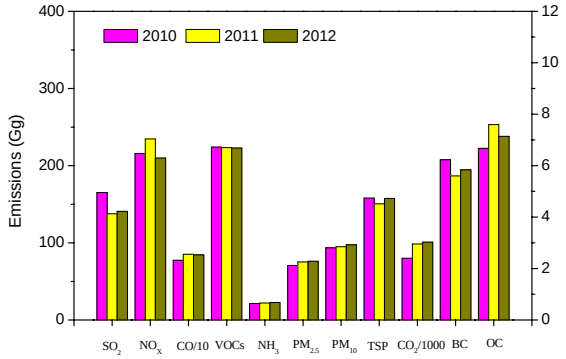

(a)

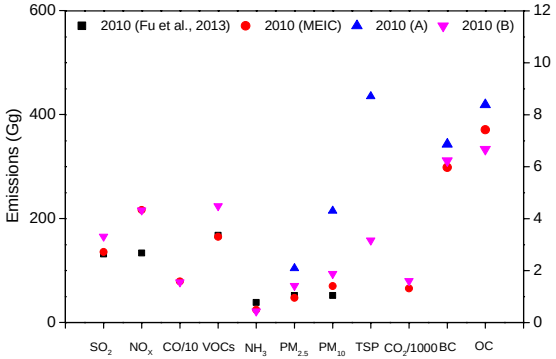

(b)

Figure 1. (a) The inter-annual variability of Nanjing emissions for 2010–2012 and **(b)** comparisons in annual emissions with other studies for 2010. The left-hand vertical axis indicates SO_2, NO_x, CO, VOCs, NH_3, $PM_{2.5}$, PM_{10}, TSP, and CO_2 while the right-hand indicates BC and OC. 2010(A) and 2010(B) refer to the emissions of current estimates with and without fugitive dust, respectively.

ACPD
15, 18691–18746, 2015

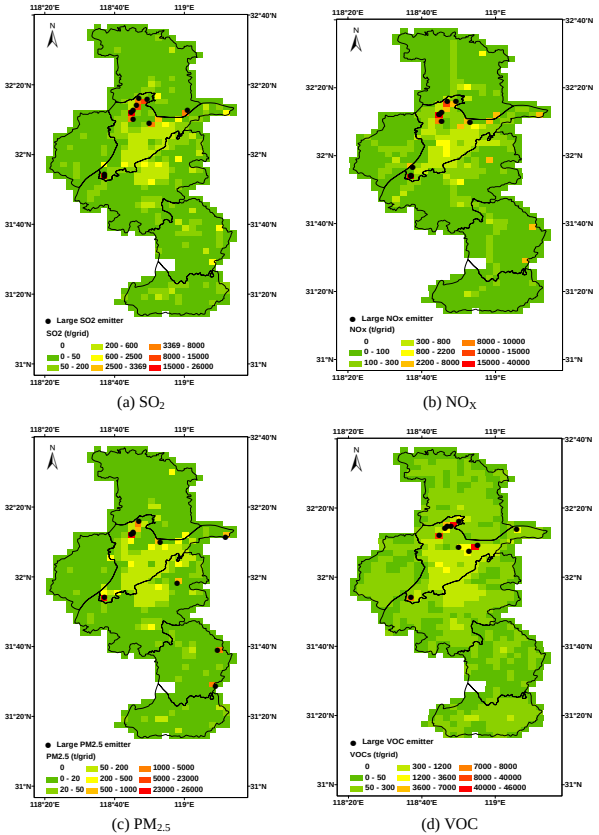

(a) SO_2 (b) NO_X

(c) $PM_{2.5}$ (d) VOC

Figure 2. Spatial distribution of emissions for Nanjing 2012, with locations of largest point sources indicated. **(a)** SO_2; **(b)** NO_x; **(c)** $PM_{2.5}$ (fugitive dust from construction and road sources excluded) and **(d)** VOC.

ACPD
15, 18691–18746, 2015

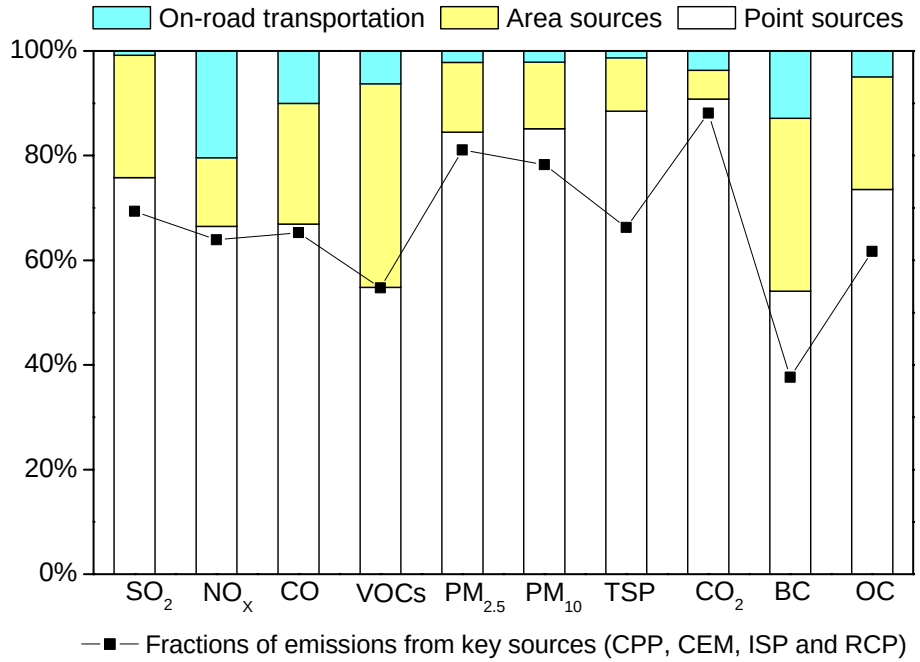

Figure 3. The emission fractions of point sources, area sources, and on-road transportation, and those of key sources of total emissions in Nanjing, 2012.

ACPD
15, 18691–18746, 2015

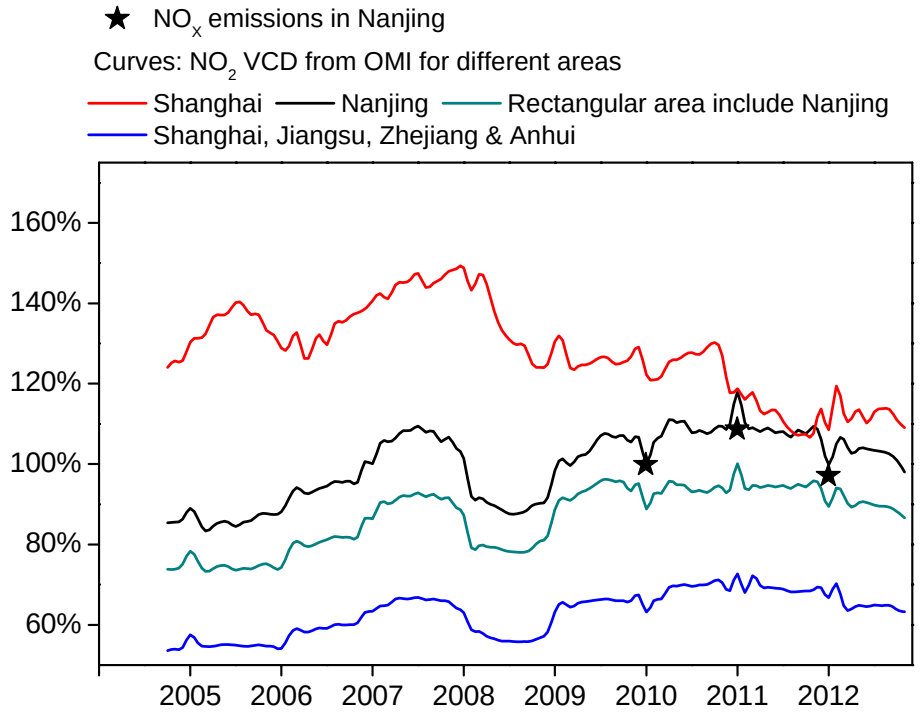

Figure 4. The inter-annual trends in NO_2 vertical column density (VCD) from OMI for selected regions (see Fig. S1a for reference) and the bottom-up NO_x emissions for 2010–2012. All the data are normalized to 2010 level in Nanjing.

ACPD
15, 18691–18746, 2015

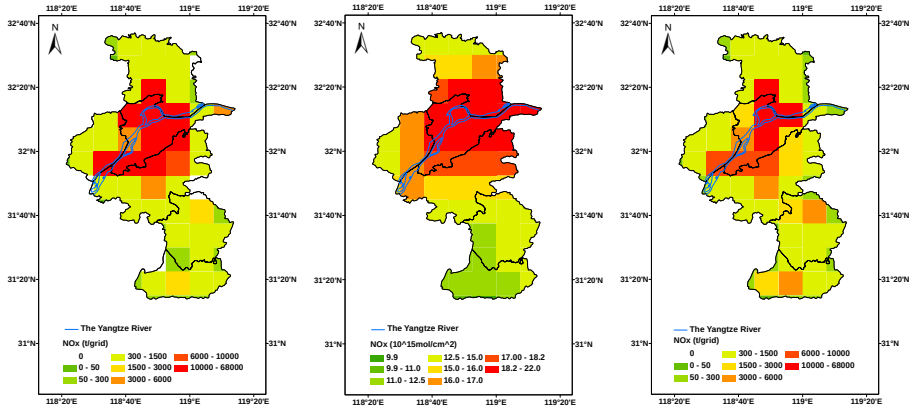

(a) Emissions: This study (b) VCD from OMI (c) Emissions: MEIC

Figure 5. (a) Spatial distribution of city-scale NO_x emissions, **(b)** summer NO_2 vertical column density (VCD) from OMI, and **(c)** NO_x emissions from MEIC for Nanjing, 2010. The resolution is $0.125^\circ \times 0.125^\circ$.

ACPD
15, 18691–18746, 2015

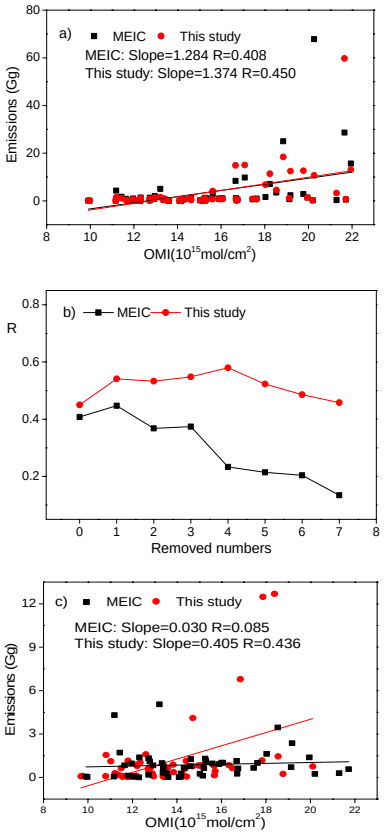

Figure 6. Spatial correlation between NO_x emissions from city- and national-scale inventories and NO_2 vertical column density (VCD) from OMI, in Nanjing, 2010 for **(a)** all grids, **(b)** step-wise exclusion of grid cells with largest emissions and **(c)** grid cells without power plant emissions.

ACPD
15, 18691–18746, 2015

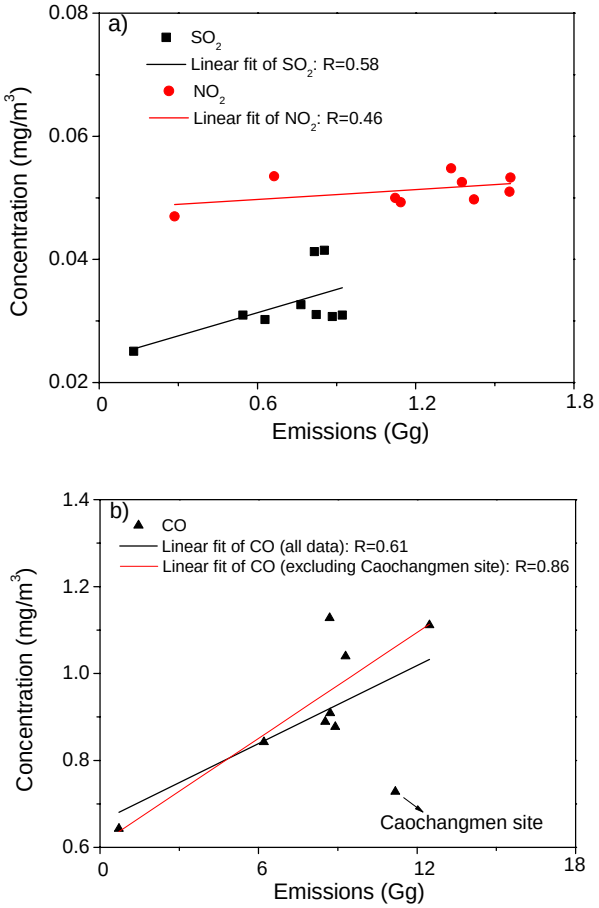

Figure 7. Linear regression of emissions and concentrations at the 9 state-operated stations in Nanjing, 2012. **(a)** SO_2 and NO_x/NO_2; **(b)** CO.

ACPD
15, 18691–18746, 2015

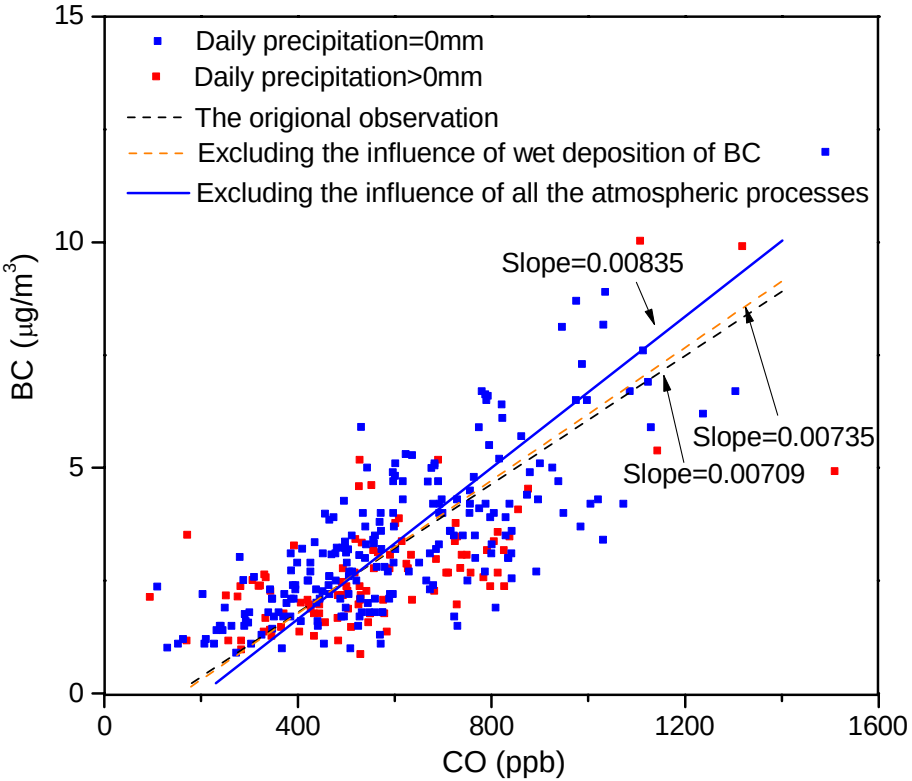

Figure 8. The correlation of daily BC and CO concentrations at Caochangmen site and the emission ratios of BC to CO from bottom-up inventories for Nanjing, 2012.

ACPD
15, 18691–18746, 2015

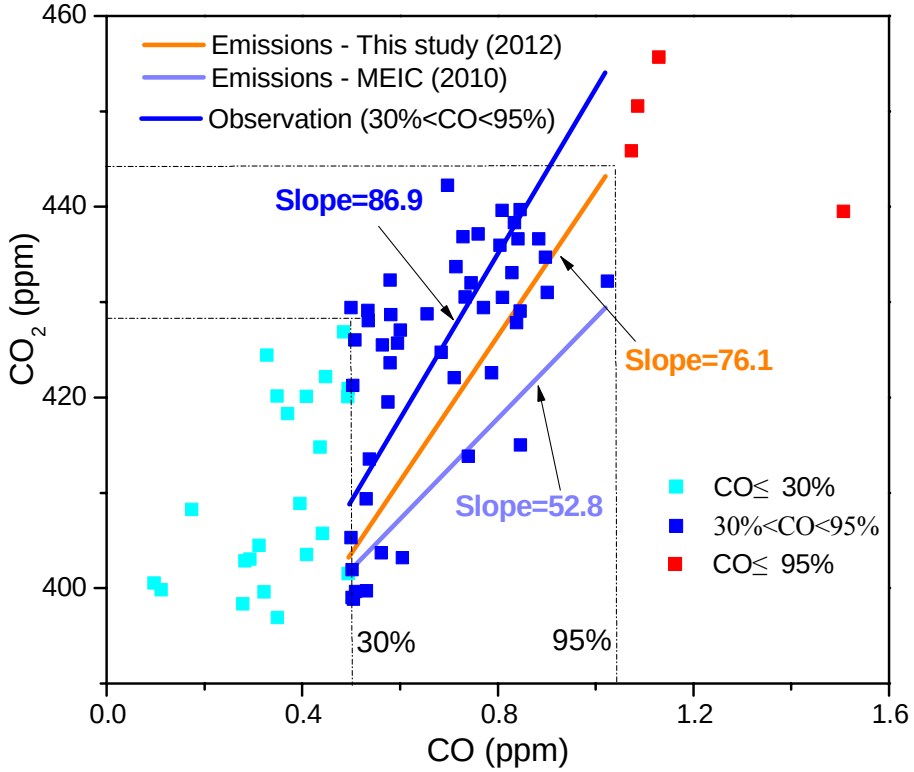

Figure 9. The correlation of daily CO_2 and CO concentrations at Caochangmen site and the emission ratios of CO_2 to CO from bottom-up inventories for Nanjing, 2012. The wintertime concentrations with CO between the 30th and 90th percentiles are used for the correlation analysis.

ACPD
15, 18691–18746, 2015

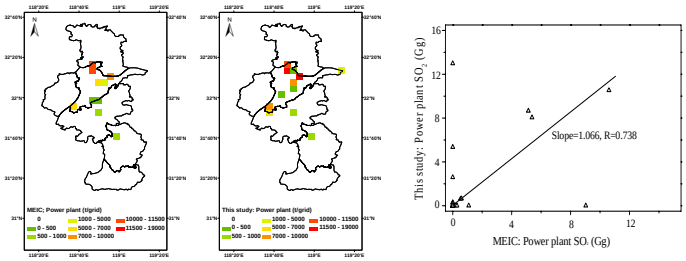

(a) Power plant: SO_2

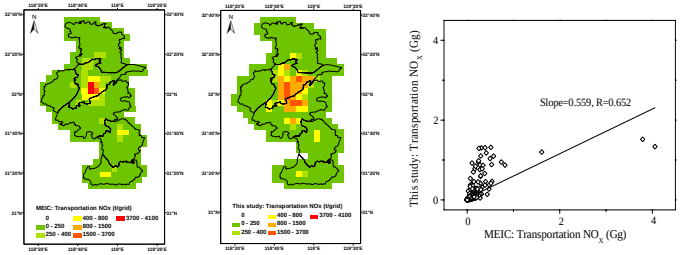

(b) Transportation: NO_X

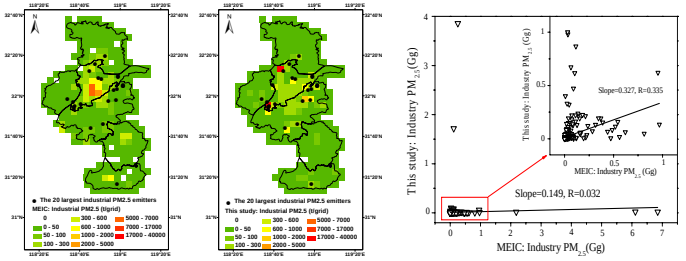

(c) Industry: $PM_{2.5}$

Figure 10. Spatial distribution and linear regression of emissions from city-scale and national inventories (MEIC) for **(a)** SO_2 from power generation, **(b)** NO_x from transportation, and **(c)** $PM_{2.5}$ from industry for Nanjing, 2010.

ACPD
15, 18691–18746, 2015